SINP/TNP/03-44/
SISSA 114/2003/EP
hep-ph/0312315

Prospects of probing θ_{13} and neutrino mass hierarchy by Supernova Neutrinos in KamLAND

Abhijit Bandyopadhyay[1], Sandhya Choubey[2,3], Srubabati Goswami[4], and Kamales Kar[1,5]
[1] *Theory Group, Saha Institute of Nuclear Physics, 1/AF, Bidhannagar, Calcutta 700 064, INDIA*
[2] *INFN, Sezione di Trieste, Trieste, Italy*
[3] *Scuola Internazionale Superiore di Studi Avanzati, I-34014, Trieste, Italy*
[4] *Harish-Chandra Research Institute, Chhatnag Road, Jhusi, Allahabad 211 019, INDIA and*
[5] *The Institute of Mathematical Sciences, C.I.T. Campus, Taramani, Chennai 600113, INDIA*

In this paper we study the physics potential of the KamLAND detector in probing neutrino oscillation parameters through observation of supernova neutrinos. In particular, we discuss the possibilities of probing the mixing angle θ_{13} and determining the sign of Δm^2_{32} from the total charged current(CC) event rates on the proton and ^{12}C target, as well as from the CC spectra. We discuss the chances of probing the earth matter effect induced modulations from the observation of CC spectra in the different CC reactions in KamLAND and find the volume required to get a statistically significant signature of the earth matter effect in different energy bins. We also calculate the event rates expected in the neutral current (NC) reactions on Carbon and free proton and investigate if the charged current to neutral current ratios, which are free of the absolute luminosity uncertainty in the supernova neutrino fluxes, can be useful in probing the oscillation parameters.

PACS numbers: 14.60.Pq, 13.15.+g

I. INTRODUCTION

KamLAND is a 1 kton liquid scintillator detector situated in the Kamioka mine in Japan. This detector is at present engaged in measuring the flux of electron antineutrinos coming from the various nuclear reactors in Japan. In 2002 it reported a phenomenal result [1], providing the clinching evidence for the Large-Mixing-Angle(LMA) MSW [2] solution to the solar neutrino problem – which was emerging as the favoured solution to explain the solar neutrino shortfall in Homestake, Kamiokande, SAGE, GALLEX/GNO [3], Super-Kamiokande(SK) [4] and the Sudbury Neutrino Observatory(SNO) [5, 6, 7] experiments. The combined two-neutrino oscillation analyses of the solar neutrino and KamLAND data including the most recent SNO salt results give the best-fit values of neutrino mass squared difference and mixing angle as $\Delta m^2_{\odot} (\equiv \Delta m^2_{21}) = 7.2 \times 10^{-5}$ eV^2, $\sin^2\theta_{\odot} (\equiv \sin^2\theta_{12}) = 0.3$ [7, 8]. The neutral current data from SNO had been instrumental in ruling out the maximal mixing and dark-side solutions ($\theta_{\odot} \geq \pi/4$), implying $\Delta m^2_{21} > 0$ [6, 9], a result now confirmed at more than 5σ level by the latest results from SNO [7, 8].

Compelling evidence in favour of neutrino oscillation have also come from the observation of up-down asymmetry in the Zenith angle distribution of atmospheric neutrinos in the SK detector. The best description to the data comes in terms of $\nu_\mu \to \nu_\tau$ ($\bar{\nu}_\mu \to \bar{\nu}_\tau$) oscillations with maximal mixing and $\Delta m^2_{atm} (\equiv \Delta m^2_{32}) = 2.0 \times 10^{-3}$ eV^2 from a recent re-analysis of data performed by the SK collaboration [11].

In the realistic three neutrino oscillation scenario the two sectors – solar and atmospheric – get coupled by the mixing angle θ_{13}, which is at present constrained by the reactor data as $\sin^2\theta_{13} \leq 0.03$ at 90% C.L. [12]. This is only an upper bound and one of the major issues to be settled by future experiments is – how small is θ_{13}. Another important question which has still not been ascertained by the current data is the sign of Δm^2_{31}. Both these issues are expected to be addressed in future long baseline experiments [13, 14]. Reactor experiments have also been shown recently to have promising capabilities to probe θ_{13} [15, 16] and under very specific demanding conditions also the sign of Δm^2_{32} [17]. A core collapse supernova (SN) in our galaxy can also play a significant role in throwing light on the above two issues [18, 19, 20]. The feasibility of supernova neutrino detection has already been demonstrated by the chance recording of the neutrino events from the supernova SN1987A by Kamiokande [21] and IMB [22] detectors. The few neutrino events detected were sufficient to confirm the basic theory of core collapse supernova and at the same time could be used to set limits on neutrino properties. SN1987A occurred in the Large Magellanic cloud at a distance of about 50 kilo parsec(kpc) from earth. For a supernova in our galactic center, we can assume a typical distance of 10 kpc and therefore expect many more neutrino events. In type II supernovae the explosion takes a few hours to penetrate through the envelope and only after that the optical and other electromagnetic signals emerge.

Whereas neutrinos start coming out right after core bounce and are therefore useful for alerting supernova telescopes. Therefore it is important that the present detectors be ready and the potentials fully explored before the next galactic supernova occurs. The capabilities of present and future detectors towards detection of neutrinos from a galactic supernova has been investigated by many authors (see e.g. [23] for a list of references). In particular, the ability of SN neutrinos to probe oscillation parameters have been considered in many papers [18, 19, 20, 24]. For example, it is shown in [18, 19, 20] that if the propagation of neutrinos is non-adiabatic in the SN matter, then they provide us a window to glean into the important parameter θ_{13}. Since both neutrino and antineutrino fluxes arrive from a SN, one can in principle also get an idea about the neutrino mass hierarchy, by observing the difference in the neutrino and antineutrino event rates in the detectors. The possibility that the neutrinos can in addition undergo earth matter effect depending on the location of the SN opens up interesting possibilities of studying earth matter effects by comparing the neutrino fluxes at different detectors [25, 26, 27, 28]. This in turn can help to distinguish between the mass hierarchies [18, 25, 26]. In a realistic picture one should consider the uncertainties coming from the SN neutrino fluxes as discussed in detail in [20]. However one can construct variables through which one can still hope to discover $2-3\sigma$ effects [1].

In this paper we do an extensive study of the KamLAND detector towards detection of SN neutrinos. The dominant reaction for detection of neutrinos in KamLAND is the $\bar{\nu}_e + p \rightarrow e^+ + n$. The liquid scintillation detector material also offers the possibility of studying the neutrino interactions on the Carbon nuclei [31]. This can proceed via both charged current – $^{12}C(\nu_e, e)^{12}N$ and $^{12}C(\bar{\nu}_e, e^+)^{12}B$ – and neutral current – $^{12}C(\nu_x, \nu_x)^{12}C^*$. The charged current reactions on ^{12}C are detected by the delayed coincidence of the final state positron/electron with the electron/positron produced by subsequent β decay of the daughter nuclei. The event signatures are separated by about tens of millisec in time and can be tagged. The final state carbon produced in the neutral current reaction on ^{12}C produces a 15.1 MeV γ – the detection of which requires large homogeneous detector volume and good energy resolution [32]. KamLAND detector satisfies both these criteria. The low energy threshold of KamLAND also makes it possible to detect the neutrino-proton elastic scattering reaction for the SN neutrinos [33]. Neutrinos and antineutrinos of all three flavors participate in this neutral current reaction and the event rate is comparable and can even be greater than the $\bar{\nu}_e + p$ events.

We explore the information that one can obtain on neutrino oscillation parameters from the observation of supernova neutrinos through the above mentioned reactions in KamLAND. Since the average energies of the $\nu_\mu/\nu_\tau(\bar{\nu}_\mu/\bar{\nu}_\tau)$ are larger than the average energies of $\nu_e(\bar{\nu}_e)$, flavor oscillations cause enrichment of the $\nu_e(\bar{\nu}_e)$ flux in higher energy neutrinos, thereby resulting in the *hardening* of the corresponding spectra. Therefore, one expects an enhancement in the CC events in presence of oscillation. This enhancement could be particularly prominent for the CC reactions on ^{12}C, for which the energy thresholds are very high and for the unoscillated ν_e or $\bar{\nu}_e$ one expects very few events. Since the degree of enhancement depends on the survival probabilities and hence on the oscillation parameters, especially the mixing angle θ_{13} and the neutrino mass hierarchy, the total observed event rates in KamLAND can be used to constrain these parameters. We study the variation of the total event rates with θ_{13} and discuss the limits on θ_{13} that one can obtain for a given mass hierarchy. We also expound the possibility of differentiating between the two hierarchies from the observation of energy integrated event rates, thereby determining the sign of Δm^2_{31}.

The hardening of the $\nu_e(\bar{\nu}_e)$ flux is also manifested in the observed electron/positron spectrum in the detector. Thus, by analysing the observed CC spectrum, one may gain information on oscillation parameters. In addition, if the SN neutrino cross the earth matter to reach the detector, then the survival probabilities would be modified due to matter effects inside the earth. This "earth regeneration" effect is dependent both on the solar neutrino oscillation parameters, as well as on θ_{13} and the hierarchy. Thus the observation of these earth modulations would also give insight into these parameters. The earth matter effect is seen as very fast oscillations superimposed on the slowly varying spectrum of the neutrinos coming from the SN. Since the variation with energy is fast, averaging effect due to energy resolution of the detector could wash out the earth effect completely from the energy spectrum. Therefore one needs a detector with very good energy resolution. KamLAND being a scintillation detector, has a very good energy resolution. We compare the degree of earth matter effect in the various CC reaction channels in KamLAND . The reactions involving the ^{12}C are seen to have large earth effect induced fluctuations in the lower energy bins. However, with the present volume of 1 kton, KamLAND lacks the statistics for drawing precise constraints from the ^{12}C spectral data. We present the minimum detector mass required to detect these modulations at a statistically significant level in various energy bins. We also present the spectrum for a 50 Kton scintillator detector and discuss the chances of probing θ_{13} and hierarchy.

Finally, we discuss the role of the uncertainties originating from our lack of knowledge of supernova neutrino fluxes.

---

[1] An alternative proposal was discussed in [29, 30], whereby using the known values of the neutrino oscillation parameters one could determine the SN parameters.

The NC reactions (both on Carbon and free proton) give a measure of the total neutrino flux coming from SN. We introduce the the ratios of charged and neutral current events in which the absolute normalisation uncertainties, e.g. due to the SN absolute luminosity or the distance of the supernova from earth, get canceled. We discuss the merits of these ratios in studying the oscillation parameters. We find that these ratios provide a good handle to probe oscillation parameters particularly when we consider the neutral current $\nu - p$ scattering reactions.

II. NEUTRINO EMISSION FROM TYPE-II SUPERNOVA

A star in an advanced stage of burning has an onion shell structure with different nuclear reactions going on in each shell. After millions of years of burning the nuclear reactions stop inside the innermost shell (i.e. the core) with matter consisting mostly of ^{56}Fe like nuclei. Once this energy generation in the core stops and if the core has mass greater than the Chandrasekhar mass, the star undergoes a very fast gravitational collapse. During this stage, electron neutrinos are produced through neutronisation reactions – electron capture on free protons and nuclei. During the early stage of the collapse, matter density of the core remains below the "neutrino trapping density" ($\sim 10^{12}$ g/cc), the neutrinos have mean free path much larger than the radius of the core and hence escape. Within a duration of tens of milliseconds, this collapse compresses the inner core of the star beyond nuclear matter densities. Consequently this inner core rebounds and creates a shock wave deep inside. This shock wave propagates radially outward through the star, gets stalled in the middle due to loss of energy through nuclear dissociation, eventually gets re-energized and finally hits the outer mantle in a few seconds, supplying an explosion energy of a few times 10^{51} ergs. This is believed to be the cause of the type II supernova explosion. During the shock phase, due to high temperature inside the core of the star, thermal ν and $\bar{\nu}$ are produced in all three flavors from e^+e^- pair production and "urca processes" [34]. This production of neutrino pairs stops when neutrino density becomes high enough so that the inverse process of pair production balances the direct process. The total energy of the neutrinos from pair production at the shock phase is much larger than that of the neutronisation neutrinos. Almost all the gravitational binding energy released due to the collapse is radiated away through these neutrinos with only a few percent going to the explosion. These neutrinos inside the core of the star are in equilibrium with the ambient matter density and their energy distributions are close to Fermi-Dirac, with the characteristic temperature given by the temperature of last scattering. This is seen through simulations and through the analysis of SN1987A neutrinos. Out of all neutrinos, ν_μ, ν_τ and their antiparticles interact with matter only through neutral current, whereas ν_e and $\bar{\nu}_e$ have both charged current and neutral current interactions. Since matter inside the SN is neutron rich, ν_e's interact more than $\bar{\nu}_e$'s. Therefore ν_μ, ν_τ and their antiparticles decouple first and hence have the largest temperature, followed by the $\bar{\nu}_e$, while ν_e decouple last and have the smallest temperature. In this paper we consider the detection of neutrinos arriving at earth from the cooling phase of the SN burst, and assume that all the three types of neutrino gas (ν_e, $\bar{\nu}_e$ and ν_x, where x stands for the four species ν_μ, $\bar{\nu}_\mu$, ν_τ and $\bar{\nu}_\tau$) have the Fermi-Dirac energy distributions with equilibrium temperatures as 11, 16 and 25 MeV respectively (see for instance [35]). However although the temperature hierarchy are generally believed to be in the above order the exact values of the average energies may differ depending on the details of supernova simulations [36, 37, 38]. Such simulations also indicate that the high energy tail of the neutrino spectra from SN is better reproduced by a "pinched" Fermi-Dirac distribution with a non-zero chemical potential [39]. Finally in this paper we have considered that the total binding energy (3×10^{53} ergs) released in the core collapse of the star is equally partitioned between various flavors. But detail simulations may give rise to scenarios where the ν_e and $\bar{\nu}_e$ luminosities can vary between (0.5-2) times the ν_x luminosity [37]. The propagation of the neutrinos and their conversion from one flavor to another depend on matter density profile in the supernova mantle. A radial profile of

$$\rho(r) = 10^{13} C \left(\frac{10Km}{r}\right)^3 \tag{1}$$

with C$\sim$ 1 - 15 provides a good description of the matter distribution for $\rho > 1$ g/cc [25, 40, 41, 42].

III. CALCULATION OF THE SURVIVAL PROBABILITY

Neutrinos and antineutrinos of all flavors are produced in a supernova burst. Before reaching the detectors, the neutrinos travel through the supernova matter, propagate through vacuum and finally may even travel through the earth's matter depending on the time of the SN burst. For the range of neutrino oscillation parameters consistent with the solar, KamLAND reactor and SK atmospheric data, one expects large matter enhanced oscillations inside the SN and regeneration effects inside the earth. The neutrino detectors on earth can detect individual fluxes of ν_e and $\bar{\nu}_e$ through the CC reactions and the combined fluxes of all the six neutrino species through the neutral current

reactions. For the case where one has only active neutrinos, it can be shown that the probabilities involved in the calculation of the event rates in the earth bound detectors are only the survival probabilities P_{ee} and $P_{\bar{e}\bar{e}}$.

In the three-generation scheme [2] neutrinos would encounter two resonances in the supernova matter. The first one corresponds to the higher atmospheric mass scale at a higher density and the second one corresponds to the lower solar mass scale at a lower matter density. The higher resonance is controlled by Δm^2_{32} and θ_{13} while the lower one is mainly controlled by Δm^2_{21} and θ_{12}. The transition probability depends crucially on the sign of the mass squared difference. Therefore depending on the sign of Δm^2_{32}, which is still completely unknown, we can have two possibilities for the neutrino mass spectrum: Normal Hierarchy (NH) when $\Delta m^2_{32} > 0$, or Inverted Hierarchy (IH) when $\Delta m^2_{32} < 0$. We briefly summarize below the expressions for the survival probabilities in the three-generation scheme of the neutrino mass spectrum, with the current allowed mass and mixing parameters and for both normal and inverted hierarchy. We use the standard Pontecorvo-Maki-Nakagawa-Sakata parametrisation for the mixing matrix [45].

A. Normal Mass Hierarchy (NH)

The mixing angles for neutrinos in matter for normal hierarchy are given as [46]

$$\tan^2 2\theta^m_{12}(r) \;=\; \frac{\Delta m^2_{21}\sin 2\theta_{12}}{\Delta m^2_{21}\cos 2\theta_{12} - \cos^2\theta_{13}A(r)} \tag{2}$$

$$\tan^2 2\theta^m_{13}(r) \;=\; \frac{\Delta m^2_{31}\sin 2\theta_{13}}{\Delta m^2_{31}\cos 2\theta_{13} - A(r)} \tag{3}$$

$A(r)$ being the matter induced term given by

$$A(r) \;=\; 2\sqrt{2}G_F N_A n_e(r) E_\nu \tag{4}$$

where G_F is the Fermi constant, N_A the Avogadro number, $n_e(r)$ the ambient electron density in the supernova at radius r and E_ν the energy of the neutrino beam. Since $A >> \Delta m^2_{31} >> \Delta m^2_{21}$ at the point of production of the neutrinos, from equations (2) and (3) we have, $\theta^m_{12} \approx \frac{\pi}{2} \approx \theta^m_{13}$, which means that neutrinos are created in pure ν^m_3 states and the expression for the survival probability is

$$P_{ee} \;=\; P_H P_L P^{\oplus}_{1e} + P_H(1-P_L)P^{\oplus}_{2e} + (1-P_H)P^{\oplus}_{3e} \tag{5}$$

where $P^{\oplus}_{ie}$ are the $\nu_i \to \nu_e$ transition probabilities and may depend on earth matter effect if neutrino cross the earth. P_H and P_L are the "jump" probabilities at the high and low density resonance transitions respectively and for these we use the standard double exponential forms [47, 48]. Although this form derived in [47] was in the context of solar neutrinos and exponential density profile, it was shown in [48] that this holds good for generic SN density profiles as well.

For antineutrinos the expressions (2) and (3) hold with the minus sign in the denominators replaced by a plus sign. Then, at the antineutrino production point $\bar{\theta}^m_{12} \approx 0 \approx \bar{\theta}^m_{13}$ (i.e. they are created in the $\bar{\nu}^m_1$ state) and the anti neutrinos the survival probabilities are given by

$$P_{\bar{e}\bar{e}} \;=\; (1-\bar{P}_L)\bar{P}^{\oplus}_{1e} + \bar{P}_L\bar{P}^{\oplus}_{2e} \tag{6}$$

where the jump probability $\bar{P}_L$ for the anti neutrinos is given by the standard expression as given in [48, 49].

B. Inverted Mass Hierarchy (IH)

For inverted mass hierarchy ($\Delta m^2_{31} \approx \Delta m^2_{32} < 0$) the 12 matter mixing angle is same as that for NH both for neutrinos and antineutrinos. The 13 mixing angle in matter is given by the same expression as for NH with the sign

---

[2] We disregard the positive evidence from LSND experiment [43]. Study of SN neutrinos in the context of four neutrino species have been done in [44]. We also neglect the CP violating phases which is a justified approximation as for equal luminosities and temperature of the μ and τ neutrinos coming from SN, the relevant probability at the detector is only the electron neutrino survival probability which does not depend on the CP phases.

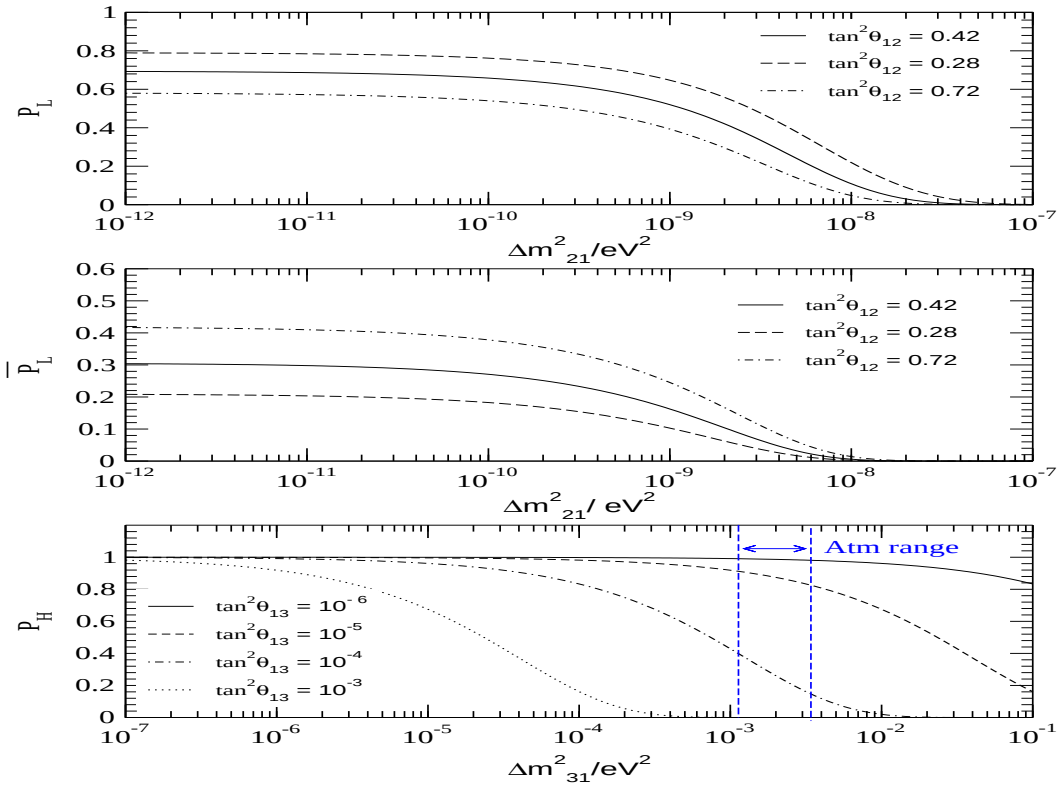

FIG. 1: $P_L, \bar{P}_L$ as a function of Δm^2_{21} and P_H as a function of Δm^2_{31} at neutrino energy $E_\nu = 20$ MeV

of Δm^2_{31} reversed. Then at the production point of the neutrino $\theta^m_{12} \approx \frac{\pi}{2}$ and $\theta^m_{13} \approx 0$ and ν_e are produced as ν^m_2 and the neutrino survival probability is

$$P_{ee} \;=\; P_L P^{\oplus}_{1e} + (1 - P_L) P^{\oplus}_{2e} \tag{7}$$

whereas at the antineutrino production point $\bar{\theta}^m_{12} \approx 0$ and $\bar{\theta}^m_{12} \approx \frac{\pi}{2}$ so that $\bar{\nu}_e$ are produced as ν^m_3 states and the survival probability is given by

$$P_{\bar{e}\bar{e}} \;=\; (1 - \bar{P}_L) P_H \bar{P}^{\oplus}_{1e} + \bar{P}_L P_H \bar{P}^{\oplus}_{2e} + (1 - P_H) \bar{P}^{\oplus}_{3e} \tag{8}$$

C. Dependence of survival probability on oscillation parameters and energy

The dependence of the jump probabilities P_L and $\bar{P}_L$ on the 1-2 mass and mixing parameters and of P_H on the 1-3 mass and mixing parameters has been shown in the figure 1, for an illustrative neutrino energy of 20 MeV. We see from this figure that for $\Delta m^2_{21} > 10^{-7}$ eV^2, $P_L = 0 = \bar{P}_L$ for all values of θ_{12}. We have checked that this conclusion remains valid for all energies of the SN neutrinos. Since KamLAND and the solar neutrino data have independently confirmed that Δm^2_{21} lies in the LMA region, we can safely take $P_L = 0$ in the expressions for the probabilities. For the current range of Δm^2_{31} allowed by the atmospheric neutrino data, P_H sharply depends on the value of θ_{13}. It is therefore useful to consider the survival probabilities in three limiting range of θ_{13} [3]

[3] In what follows, we keep $\sin^2\theta_{12}$ fixed at its current best-fit value of 0.3, and Δm^2_{31} fixed at 0.002, the best-fit value presented by the latest re-analysis of the SK atmospheric collaboration. The probabilities depend on Δm^2_{21} if there are earth matter effects, and we keep Δm^2_{21} fixed at its best-fit value of $7.2 \times 10^{-2} eV^2$.

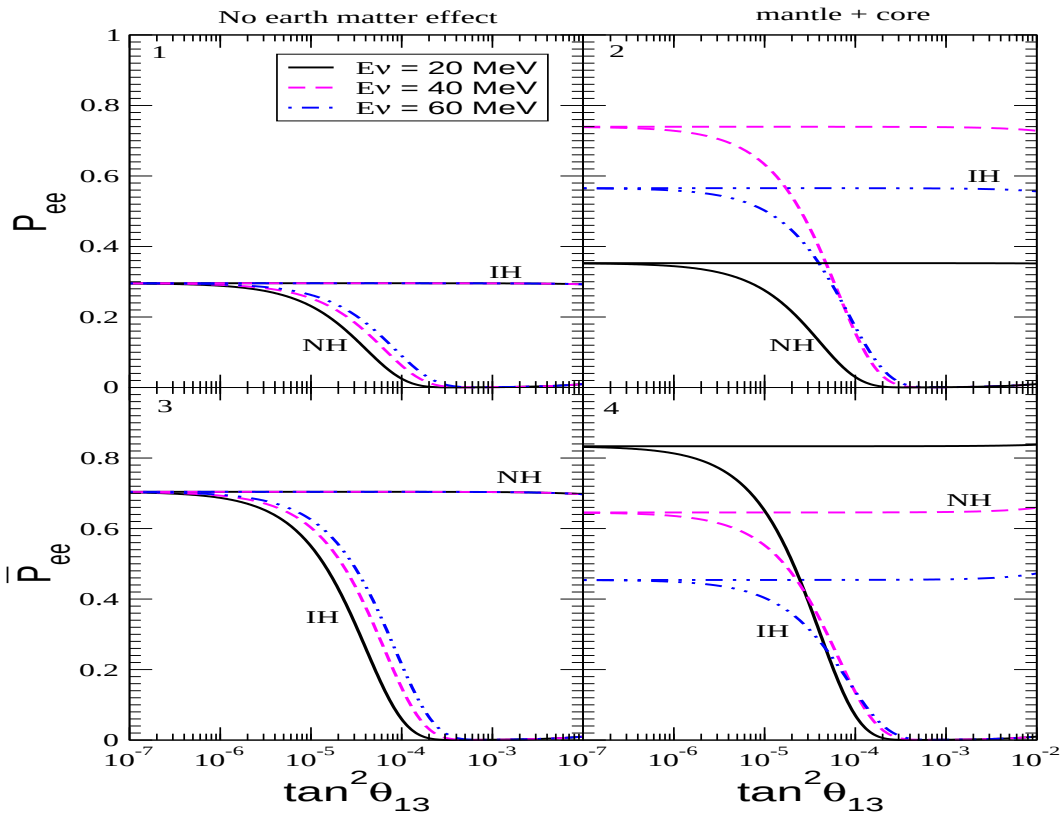

FIG. 2: Plot of P_{ee}^{NH}, $P_{\bar{e}\bar{e}}^{NH}$, P_{ee}^{IH} and $P_{\bar{e}\bar{e}}^{IH}$ vs $\tan^2\theta_{13}$ for three different values of neutrino energy. The left-hand panels show the case for neutrinos coming straight from the SN while the right-hand panels correspond to the case when they travel earth's mantle and core as well. The other oscillation parameters are kept fixed at their current best-fit values.

- *The small θ_{13} range*: For $\tan^2\theta_{13} \lesssim 10^{-6}$, $P_H = 1$ practically over the whole relevant energy range of the SN neutrinos, except for very small energies. This is the regime of extreme non-adiabatic transitions.
- *The intermediate θ_{13} range*: In the range $10^{-6} \lesssim \tan^2\theta_{13} \lesssim 10^{-3}$, P_H ranges between 0 and 1, depending on the exact value of θ_{13} and energy.
- *The large θ_{13} range*: For $\tan^2\theta_{13} \gtrsim 10^{-3}$ $P_H = 0$ for all energies, in the entire range of Δm^2_{31} allowed by the atmospheric neutrino data. This is the region of complete adiabatic propagation.

1. *No earth matter effect*

For this case

$$P_{1e}^{\oplus} = \cos^2\theta_{13}\cos^2\theta_{12} \quad (9)$$
$$P_{2e}^{\oplus} = \cos^2\theta_{13}\sin^2\theta_{12} \quad (10)$$
$$P_{3e}^{\oplus} = \sin^2\theta_{13} \quad (11)$$

Depending on the value of θ_{13}, the probabilities assume the following forms:

- In the range $\tan^2\theta_{13} \lesssim 10^{-6}$, $P_H = 1$, $\sin^2\theta_{13} \approx 0$ so that,

$$P_{ee}^{NH} = \sin^2\theta_{12} = P_{ee}^{IH} \quad (12)$$
$$P_{\bar{e}\bar{e}}^{NH} = \cos^2\theta_{12} = P_{\bar{e}\bar{e}}^{IH} \quad (13)$$

- In the range $10^{-6} \lesssim \tan^2\theta_{13} \lesssim 10^{-3}$, P_H is non-zero but $\sin^2\theta_{13}$ can be taken as zero and,

$$P_{ee}^{NH} = P_H \sin^2\theta_{12}; P_{ee}^{IH} = \sin^2\theta_{12} \quad (14)$$
$$P_{\bar{e}\bar{e}}^{NH} = \cos^2\theta_{12}; P_{\bar{e}\bar{e}}^{IH} = P_H \cos^2\theta_{12} \quad (15)$$

- For $\tan^2\theta_{13} \gtrsim 10^{-3}$, $P_H = 0$, $\sin^2\theta_{13}$ can be non-zero [4] and the probabilities are,

$$P_{ee}^{NH} = \sin^2\theta_{13} \quad ; \quad P_{ee}^{IH} = \cos^2\theta_{13}\sin^2\theta_{12} \quad (16)$$
$$P_{\bar{e}\bar{e}}^{NH} = \cos^2\theta_{13}\cos^2\theta_{12} \quad ; \quad P_{\bar{e}\bar{e}}^{IH} = \sin^2\theta_{13} \quad (17)$$

The dependence of the probabilities on θ_{13} for the case of no earth matter effects are shown in the left-hand panels of figure 2, for three different values of the neutrino energy. From the figure 2 and the equations for the probabilities at various limits we note the following points:

1. In the small θ_{13} regime ($\tan^2\theta_{13} \lesssim 10^{-6}$) the survival probabilities for both ν_e and $\bar{\nu}_e$ are independent of the value of θ_{13} and neutrino energy. The flavor conversion is governed only by the solar mixing angle θ_{12}, and one cannot distinguish between normal and inverted hierarchies in either the neutrino or the antineutrino channel.

2. For IH(NH) the survival probabilities for $\nu_e(\bar{\nu}_e)$ do not depend on P_H. Hence they remain largely independent of the value of θ_{13} and the neutrino energy and depend mainly on the solar mixing angle θ_{12} in the entire oscillation parameter range considered in this paper. Dependence on θ_{13} comes only for NH(IH) in the $\nu_e(\bar{\nu}_e)$ channel.

3. In the intermediate θ_{13} range ($10^{-6} \lesssim \tan^2\theta_{13} \lesssim 10^{-3}$) and with NH(IH) as the true mass hierarchy, the neutrino(anti-neutrino) survival probabilities depend sharply on the value of θ_{13} and neutrino energy, through the dependence of P_H on these variables.

4. In the large θ_{13} range ($\tan^2\theta_{13} \gtrsim 10^{-3}$) and with NH(IH) as the true mass hierarchy, the neutrino(anti-neutrino) survival probabilities are very small, within the CHOOZ limit of $\sin^2\theta_{13}$, and do not depend on energy.

5. In the case of $\nu_e(\bar{\nu}_e)$ for NH(IH), the survival probabilities decrease from $\sin^2\theta_{12}(\cos^2\theta_{12})$ to $\sim \sin^2\theta_{13}(\sin^2\theta_{13})$, as $\tan^2\theta_{13}$ changes from $\sim 10^{-6}$ to $\sim 10^{-3}$. Since the best-fit value of the solar mixing angle is $\sin^2\theta_{12} \approx 0.3$, $P_{\bar{e}\bar{e}}^{IH}$has a much sharper decrease with $\tan^2\theta_{13}$ than P_{ee}^{NH} . Therefore the $\bar{\nu}_e$ events could be expected to have better sensitivity to θ_{13} on this count.

6. In the range $10^{-6} \lesssim \tan^2\theta_{13} \lesssim 10^{-3}$, P_{ee}^{NH} and $P_{\bar{e}\bar{e}}^{IH}$ depend on Δm^2_{31} through P_H but over the currently allowed atmospheric range of this parameter, the dependence is not very strong.

7. The survival probabilities in general depend on the value of θ_{12}, excepting P_{ee}^{NH} and $P_{\bar{e}\bar{e}}^{IH}$in the large θ_{13} regime, but there is no dependence of the probabilities on Δm^2_{21}.

2. Including the earth matter effect

For this case

$$P_{1e}^{\oplus} = \cos^2\theta_{13}|A_{1e}^{\oplus}(2gen)|^2 \quad (18)$$
$$P_{2e}^{\oplus} = \cos^2\theta_{13}|A_{2e}^{\oplus}(2gen)|^2 \quad (19)$$
$$P_{3e}^{\oplus} = \sin^2\theta_{13} \quad (20)$$

$A_{1e}^{\oplus}$(2gen) and $A_{2e}^{\oplus}$(2gen) are the $\nu_i \to \nu_e$ transition amplitudes inside earth for two generations [50, 51], with matter term $A(r)$ replaced by $A(r)\cos^2\theta_{13}$. Since the supernova neutrinos have typical energy of $\sim$ 10 MeV the matter potential in the earth is << the high mass scale Δm^2_{31}. However, oscillations due to the Δm^2_{21} scale are affected by the earth matter effect.

---

[4] However if we restrict ourselves up to the CHOOZ bound then $\sin^2\theta_{13}$ stays very small.

- For $\tan^2\theta_{13} \lesssim 10^{-6}$, $P_H = 1$, $\sin^2\theta_{13}$ can be set to zero and the probabilities are,

$$P_{ee}^{NH} = P_{2e}^{\oplus}(2gen) = P_{ee}^{IH} \tag{21}$$
$$P_{\bar{e}\bar{e}}^{NH} = \bar{P}_{1e}^{\oplus}(2gen) = P_{\bar{e}\bar{e}}^{IH} \tag{22}$$

- For $10^{-6} \lesssim \tan^2\theta_{13} \lesssim 10^{-3}$ the probabilities can be written as,

$$P_{ee}^{NH} \approx P_H P_{2e}^{\oplus} \quad ; \quad P_{ee}^{IH} \approx P_{2e}^{\oplus} \tag{23}$$
$$P_{\bar{e}\bar{e}}^{NH} \approx \bar{P}_{1e}^{\oplus} \quad ; \quad P_{\bar{e}\bar{e}}^{IH} \approx P_H P_{1e}^{\oplus} \tag{24}$$

  where we have used $\sin^2\theta_{13} = 0$ which is a good approximation in this range.

- For $\tan^2\theta_{13} \gtrsim 10^{-3}$, $\sin^2\theta_{13}$ may be small but non-zero in the range allowed by the CHOOZ results. However as we have seen before that $P_H = 0$ and the probabilities are,

$$P_{ee}^{NH} = \sin^2\theta_{13} \quad ; \quad P_{ee}^{IH} = P_{2e}^{\oplus} \tag{25}$$
$$P_{\bar{e}\bar{e}}^{NH} = \bar{P}_{1e}^{\oplus} \quad ; \quad P_{\bar{e}\bar{e}}^{IH} = \sin^2\theta_{13} \tag{26}$$

We can define the following quantities valid for all values of θ_{13}:

$$R_{ee}^{NH} = P_H \cos^2\theta_{13} f_{reg} \quad ; \quad R_{ee}^{IH} = \cos^2\theta_{13}\ f_{reg} \tag{27}$$
$$R_{\bar{e}\bar{e}}^{NH} = -\cos^2\theta_{13}\ \bar{f}_{reg} \quad ; \quad R_{\bar{e}\bar{e}}^{IH} = -P_H \cos^2\theta_{13}\ \bar{f}_{reg} \tag{28}$$

where $R_{ii}^{x} = P_{ii}^{x}$(with earth effect) - P_{ii}^{x}(without earth effect), i can be e or $\bar{e}$ and x can be NH or IH and

$$f_{reg} = |A_{2e}^{\oplus}|^2 - \sin^2\theta_{12} \tag{29}$$
$$\bar{f}_{reg} = |\bar{A}_{2e}^{\oplus}|^2 - \sin^2\theta_{12} \tag{30}$$

The f_{reg} and $\bar{f}_{reg}$ carry the information about the regeneration effects inside the earth and are dependent on the neutrino energy, θ_{12} and Δm^2_{21}.

From Eqs. (27) and (28) we see that while R_{ee}^{IH} and $R_{\bar{e}\bar{e}}^{NH}$ are independent of P_H, R_{ee}^{NH} and $R_{\bar{e}\bar{e}}^{IH}$ are linearly proportional to it. Thus, while the $\bar{\nu}_e(\nu_e)$ spectrum will have an energy (and θ_{12} and Δm^2_{21}) dependent, but largely θ_{13} independent modulation induced by $\bar{f}_{reg}(f_{reg})$ for NH(IH), for IH(NH) the degree of earth matter effects will depend sharply on the value of θ_{13}. In particular, when $P_H = 1$ the earth effects will be same for both the hierarchies. However, as θ_{13} increases, P_H decreases, resulting in smaller earth regeneration effect in the $\bar{\nu}_e(\nu_e)$ spectrum for IH(NH). The earth effect completely vanishes in the $\bar{\nu}_e(\nu_e)$ channel for IH(NH) when $P_H = 0$ for $\tan^2\theta_{13} \gtrsim 10^{-3}$.

We show the impact of earth matter effect on the survival probabilities in the right-hand panels of figure 2. From the expressions above and figure 2 we note the following points in this case:

1. In the small θ_{13} regime ($\tan^2\theta_{13} \lesssim 10^{-6}$), the probabilities are again independent of θ_{13} but they are not independent of energy anymore, as the earth matter effect introduces some energy dependence. Apart from θ_{12} the probabilities in this regime are now also functions of Δm^2_{21} through the dependence on f_{reg} and $\bar{f}_{reg}$. However as is clear from figure 2 and Eqs. (21) and (22) the probabilities are same for both hierarchies and introduction of earth effect does not help in lifting the degeneracy of the probabilities between normal and inverted hierarchies.

2. As can be seen clearly from figure 2, $P_{\bar{e}\bar{e}}^{NH}$and P_{ee}^{IH} become energy dependent with the inclusion of earth matter effect but for a fixed energy there is no dependence of these probabilities on θ_{13}.

3. In the intermediate θ_{13} range ($10^{-6} \lesssim \tan^2\theta_{13} \lesssim 10^{-3}$) for the $\bar{\nu}_e(\nu_e)$ channel with IH(NH) as the true mass hierarchy, the θ_{13} dependence is governed by P_H. Whereas the energy dependence of the the neutrino(anti-neutrino) survival probabilities is due to both P_H and the earth regeneration factor $\bar{f}_{reg}(f_{reg})$. Since the amount of earth regeneration for these channels depends on P_H (cf. Eq. (28)) the degree of energy dependence is different for different ranges of θ_{13} – there being more earth matter induced energy variation at smaller θ_{13} as can be seen in figure 2.

4. For large values of θ_{13} ($\tan^2\theta_{13} \gtrsim 10^{-3}$) P_{ee}^{NH} and $P_{\bar{e}\bar{e}}^{IH}$are given by the same expressions as the no earth effect case and do not depend on energy or earth matter effects. But P_{ee}^{IH} and $P_{\bar{e}\bar{e}}^{NH}$depend on earth matter effect and energy.

IV. SUPERNOVA NEUTRINO SIGNAL IN THE KAMLAND DETECTOR

A. Energy integrated event rates in KamLAND

Neutrinos from a SN can be observed in KamLAND through their charged and neutral current reactions with the detector scintillator material. The total number of charged current events triggered by the SN $\bar{\nu}_e$ flux arriving at KamLAND can be expressed as,

$$\begin{aligned} R^{CC} &= \eta N \times \int dE_{vis} \int dE_\nu \sigma(E_\nu) R(E_{vis}, E_\nu) \sigma_{CC}(E_\nu) \\ &\times \Big[F_{\bar{e}}(E_\nu) P_{\bar{e}\bar{e}}(E_\nu) + F_{\bar{x}}(E_\nu)(1 - P_{\bar{e}\bar{e}}(E_\nu)) \Big] \end{aligned} \tag{31}$$

where N is the number of target nuclei/nucleons, η is the detection efficiency, $\sigma_{CC}(E_\nu)$ are the corresponding CC cross-sections for the $\bar{\nu}_e$ and E_{vis} is the measured *visible* energy of the emitted positron, when the true visible energy, E^T_{vis} is related to the antineutrino energy E_ν as, $E^T_{vis} \cong E_\nu - 0.78$ MeV. $R(E_{vis}, E_{e^+})$ is the Gaussian energy resolution function of the detector given by,

$$R(E_{vis}, E_{e^+}) = \frac{1}{\sqrt{2\pi\sigma_0^2}} \exp\left(-\frac{(E_{vis} - E_{e^+} - m_e)^2}{2\sigma_0^2} \right) \tag{32}$$

with $\sigma_0(E)/\mathrm{E} = 7.5\%/\sqrt{(E)}$ as given by the KamLAND collaboration [1]. $F_{\bar{e}}$ is the unoscillated electron antineutrino flux produced in the SN and $F_{\bar{x}}$ stands for the flux of any of the other antineutrino flavors, $\bar{\nu}_\mu$ or $\bar{\nu}_\tau$. The expression for the neutrino flux of species α, arriving at the detector is given by

$$F_\alpha(E_\nu, L_\alpha, T_\alpha, d) = \frac{L_\alpha}{4\pi d^2} \times \frac{E_\nu^2}{5.68 T_\alpha^4 \left[\exp(\frac{E_\nu}{T_\alpha}) + 1 \right]} \tag{33}$$

where L_α is the total SN energy released in the neutrino species ν_α, T_α is the temperature of the ν_α gas at the neutrino sphere and d is the distance of the supernova from earth. In Eq.(33) we assume a pure Fermi-Dirac spectrum for the neutrinos. As discussed before in section II, the actual SN neutrino spectrum may deviate from a perfect black body. This deviation can be accounted for by introducing in the neutrino distribution function a "pinching factor" η, which is a dimensionless parameter defined as μ_α/T_α, where μ_α and T_α are the chemical potential and the temperature of the neutrino species ν_α [39]. The pinching factor has the effect of suppressing the high energy end of the neutrino spectrum [5].

The number of CC events induced by the SN ν_e in KamLAND is given by the same expression Eq.(31), but with the antineutrino fluxes $F_{\bar{e}}$ and $F_{\bar{x}}$ replaced by the neutrino fluxes F_e and F_x, $P_{\bar{e}\bar{e}}$ replaced by P_{ee} and with the corresponding CC interaction cross-section for the neutrinos. The expression for the neutral current events in the detector is given by

$$\begin{aligned} R^{NC} &= \eta N \int dE_\nu \\ &\times \Big[\sigma_{NC}(E_\nu) \Big(F_e(E_\nu) + 2F_x(E_\nu) \Big) + \bar{\sigma}_{NC}(E_\nu) \Big(F_{\bar{e}}(E_\nu) + 2F_{\bar{x}}(E_\nu) \Big) \Big] \end{aligned} \tag{34}$$

where $\sigma_{NC}(E_\nu)$ and $\bar{\sigma}_{NC}(E_\nu)$ are the NC cross-sections corresponding to neutrinos and antineutrinos respectively and all other variable are as defined before.

B. Detection reactions in KamLAND

KamLAND is an isoparrafin based liquid scintillator (80% paraffin oil and 20% pseudodocumene) detector with a typical composition of C_nH_{2n}. The main CC detection reactions in KamLAND are:

---

[5] Consequences of a a small deviation from Fermi-Dirac in the high energy tail, for neutrino oscillation parameters, have been discussed for instance in [20].

1. The CC capture of $\bar{\nu}_e$ on free protons:

$$\bar{\nu_e} + p \rightarrow e^+ + n \tag{35}$$

The threshold $\bar{\nu}_e$ energy for this reaction is 1.8 MeV. The released positron annihilates with an ambient electron to produce two gamma rays. The final state neutron thermalises in about 180 μsec to produce a 2.2 MeV γ ray. The delayed coincidence of these γs gives an event grossly free from backgrounds. [6].

2. The CC capture of $\bar{\nu}_e$ on ^{12}C:

$$\bar{\nu_e} + ^{12}C \rightarrow ^{12}B + e^+ \tag{36}$$
$$^{12}B \rightarrow ^{12}C + e^- + \bar{\nu_e} \tag{37}$$

The threshold antineutrino energy for the capture on ^{12}C is 14.39 MeV. The β unstable ^{12}B eventually decays with a half life of $\tau_{1/2} = 20.20$ ms. This signal is also recorded by the delayed coincidence of the γs produced from annihilation of e^+ produced in the final state of the first reaction, followed by the annihilation of e^- produced in the final state of the second reaction.

3. The CC capture of ν_e on ^{12}C:

$$\nu_e + ^{12}C \rightarrow ^{12}N + e^- \tag{38}$$
$$^{12}N \rightarrow ^{12}C + e^+ + \nu_e \tag{39}$$

The threshold neutrino energy for capture on ^{12}C is 17.34 MeV and the β unstable ^{12}N created in this process decays with a half life of $\tau_{1/2} = 11.00$ ms. The signal is again recorded by the delayed coincidence of the two γs produced from annihilation of the e^+ and e^- respectively, produced in the final states of the two above reactions.

The main NC reactions by which KamLAND can observe SN neutrinos are:

1. The neutrino-proton elastic scattering:

$$\nu + p \rightarrow \nu + p \tag{40}$$

The scattered protons have kinetic energies of $\sim$ MeV and hence cannot be observed in the high-threshold Cerenkov detectors. However in a scintillator detector like KamLAND, the energy deposition due to the protons can be observed in spite of the quenching of the proton energy due to ionisation [33]. The cross-section for ν_e scattering is same as that of scattering by ν_x, while the cross-section for $\bar{\nu}_e$ scattering is same as that of scattering by $\nu_{\bar{x}}$ [33]. But the scattering cross-section of the particles is different from the scattering cross-section of the anti-particles. However under the approximation of $E_\nu/M_p << 1$, where M_p is the proton mass, even the particle and anti-particle cross-sections can be taken as almost equal.

2. Neutral Current break-up of ^{12}C:

$$\nu(\bar{\nu}) + ^{12}C \rightarrow ^{12}C^* + \nu'(\bar{\nu'}) \tag{41}$$
$$^{12}C^* \rightarrow ^{12}C + \gamma(15.11MeV) \tag{42}$$

The threshold energy for this reaction is 15.11 MeV. The detection of the 15.11 MeV γ released by the de-excitation of the $^{12}C^*$ gives an unambiguous signal of the supernova neutrinos, virtually free from all backgrounds.

All the above reactions have distinctive signatures, allowing one to count the event rates separately. The CC reactions can also measure the energy spectrum of the final state electrons/positrons. In the $\nu - p$ NC scattering reaction, the scattered proton carries the energy information and hence this reaction also has sensitivity to the spectrum of the incoming neutrinos. However for the NC break-up of ^{12}C, the emitted photon has no information about the neutrino energy and this is the only reaction in KamLAND with no energy sensitivity. We take the $\bar{\nu}_e + p$ absorption cross-section from [52], the $\nu - p$ elastic scattering cross-section from [33] and the ^{12}C reaction cross-sections from [53].

---

[6] This is the reaction used by KamLAND to detect the reactor antineutrinos

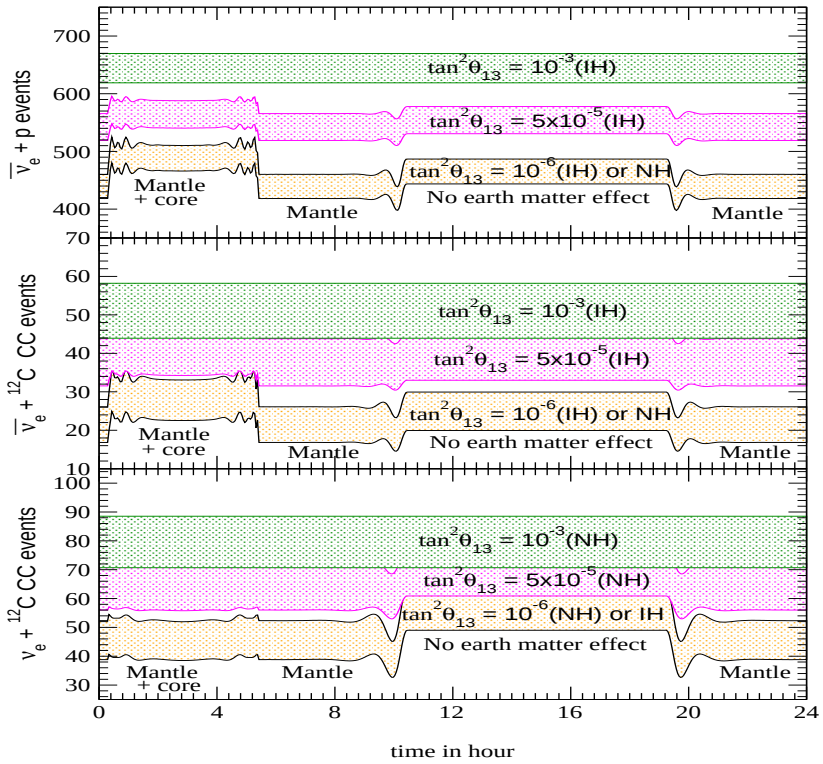

FIG. 3: Plot of the event rates with 1σ statistical error bands in the different CC reaction in KamLAND as a function of time of occurrence of the Supernova for different values of θ_{13}. The curves are drawn with Δm^2_{21} and θ_{12} fixed at the best-fit value from the global solar and KamLAND data. See text for details.

Finally a note on the expected backgrounds in KamLAND. The Kamioka mine has a rock overburden of 2700 m.w.e producing 0.34 Hz of cosmic-ray muons. Since the SN neutrino signal lasts for about 10 s, the signal for the $\bar{\nu_e} + p$ events is $\sim 300/10 = 30$ Hz, while that for the Carbon events are $10/10 = 1$ Hz. Thus the signal is greater than the cosmic ray backgrounds. Since the CC reactions are observed through delayed coincidence techniques, therefore they are grossly free of background problems. The only problem may come from low-energy radioactive backgrounds for the $\nu - p$ scattering reaction. However Borexino has already demonstrated that it is possible to understand this background. If the KamLAND collaboration want to pursue the low-energy solar neutrino program then they also have to understand this background properly. However it should be noted that since the SN neutrino signals last for about 10 s and hence is a time varying signal the background for these is almost 3 times lower than the solar neutrino background [33].

C. Supernova neutrino signal in KamLAND

The total number of CC and NC event rates in KamLAND for the different reactions listed in the previous subsection, can be obtained from the Eqs. (31) and (34). In Table I we present the total number of events expected in 1 kton of detector mass with 100% assumed efficiency, induced by a galactic supernova at a distance of 10 kpc and located at the galactic centre with $\delta_s = -28.9^\circ$ (see Appendix). The lowest row in Table I gives the number of events for the case of no oscillations. Also given are the changed number of events in presence of oscillation, for both normal and inverted mass hierarchy, and for three different representative values of θ_{13}, chosen from the three interesting ranges discussed in the previous section. For events with oscillations, we present results obtained both with and without earth matter effects. The earth matter effects depend on the trajectory of the SN neutrino beam through the earth and hence on the direction of the SN from the detector. The direction of the SN with respect to the detector depends

$\tan^2\theta_{13}$	$\bar{\nu}_e$+p→n+e$^+$				ν_e+^{12}C→^{12}N+e$^+$				$\bar{\nu}_e$+^{12}C→^{12}B+e$^+$				ν+^{12}C →^{12}C*+ν	ν+p scatt.
	no earth effect		with earth effect		no earth effect		with earth effect		no earth effect		with earth effect			
	NH	IH	NH	IH	NH	IH	NH	IH	NH	IH	NH	IH		
10^{-6}	463	463	487	487	56	56	45	45	25	25	27	27	44	676
5×10^{-5}	463	554	487	564	69	56	64	45	25	39	27	41		
10^{-3}	463	644	487	644	80	56	80	45	25	51	27	51		
No osc.	383				2.6				13					

TABLE I: The number of events for the different reactions in KamLAND in presence and absence of oscillation. For the case with oscillation we present the events for three different values of θ_{13} and for both normal and inverted hierarchy. The NC events are unaffected by oscillation.

on δ_s, as well as the time during the day when the supernova explodes. In Table I the number of events presented with earth matter effect correspond to a typical time instant for which the neutrinos cross both the earth's mantle and core. Figure 3 shows the variation of the SN signal in the detector as a function of the time at which the supernova neutrinos arrive. The number of events for the CC reactions in KamLAND are shown in figure 3 for the three typical values of θ_{13}. For $\tan^2\theta_{13} = 10^{-6}$ the $\bar{\nu}_e$ and ν_e events correspond to both Normal and Inverted hierarchy. As we increase θ_{13} the number of $\bar{\nu}_e(\nu_e)$ events for NH(IH) does not change and continue to be given by the same band. The events for higher θ_{13} values correspond to the case of inverted hierarchy for the case of $\bar{\nu}_e$ events and normal hierarchy for the case of the ν_e CC capture on ^{12}C. We refer the reader to Appendix A for the details of the geometry of the neutrino trajectory inside the earth, which is used for the calculation of the number of events in the presence of earth matter effects throughout this paper.

The no oscillation number of events for the $\bar{\nu}_e + p$ absorption is 383 events while the $\nu - p$ elastic scattering gives 676 events. The cross-section for the $\nu - p$ NC scattering reaction is about 4 times lower than the $\bar{\nu}_e + p$ CC absorption reaction. But since all the six neutrino species take part in the former and since the ν_μ and ν_τ are more energetic than $\bar{\nu}_e$, one gets a larger number of $\nu - p$ elastic scattering events for the case of no oscillation. For the $\nu - p$ events presented in Table I we have ignored energy threshold effects. If we assume a threshold of 0.28 MeV, determined mainly by the radioactive backgrounds, then the number of no oscillation events for the $\nu - p$ elastic scattering reduces to 270. The energy threshold for the ^{12}C reactions are very high and so there are very few events in absence of oscillations.

Neutrino flavor oscillations convert higher energy $\nu_\mu/\nu_\tau(\bar{\nu}_\mu/\bar{\nu}_\tau)$ into $\nu_e(\bar{\nu}_e)$, resulting in an enhancement of the charged current events. The $\bar{\nu}_e + p$ CC events increase by a factor of about 1.2 – 1.7, depending on the value of θ_{13} and the neutrino mass hierarchy. The number of ^{12}C CC events increase dramatically with the introduction of neutrino flavor conversion. The $\nu_e - ^{12} C$ events increase by a factor of $\sim 17 - 30$, while $\bar{\nu}_e - ^{12} C$ events could see an increase of $\sim 2 - 4$ times, over the no oscillation expected rate. From the Table I we see that the extent of the increase in the number of events for a particular reaction channel depends on the value of θ_{13} and the neutrino mass hierarchy. However, for a given θ_{13} and hierarchy, the difference between the degree of enhancement as a result of oscillations for different reactions can be understood in terms of: (i) relative change in the average energy of the $\nu_e/\bar{\nu}_e$ flux due to flavor oscillations and (ii) degree of dependence of the CC cross-section on the neutrino energy. The relative change in the average energy due to oscillations for ν_e is much larger than that for $\bar{\nu}_e$. This explains why the ν_e events show a larger enhancement than the $\bar{\nu}_e$ events. Between the $\bar{\nu}_e$ events, we note that the relative increase for $\bar{\nu}_e - ^{12} C$ reaction is more than for $\bar{\nu}_e + p$. This is because the cross-section for the $\bar{\nu}_e - ^{12} C$ has a sharper dependence on energy than the $\bar{\nu}_e + p$ cross-section. The neutral current event rate is invariant under neutrino oscillations since the NC reactions are flavor blind.

V. PROBING θ_{13} AND MASS HIERARCHY

A. Using total event rates

From the Table I and figure 3 we observe that the increase in number of the ν_e events for normal hierarchy and the $\bar{\nu}_e$ events for inverted hierarchy depend on the value of θ_{13}. Therefore the total number of events observed may be used to probe θ_{13} and hierarchy.

The figure 4 plots the total number of $\bar{\nu}_e + p$ and the ^{12}C CC events observed in KamLAND as a function of

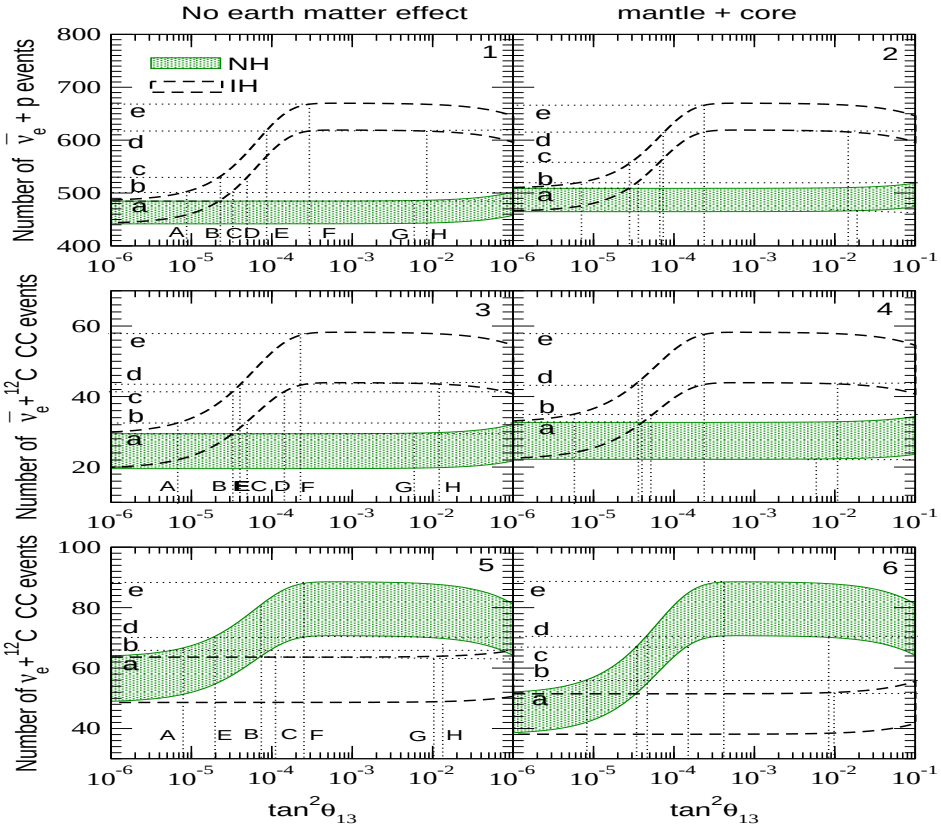

FIG. 4: Plot of the CC event rates as a function of θ_{13} for NH and IH for KamLAND. The 1σ statistical error band is also presented. See text for details.

$\tan^2\theta_{13}$ for the case with no earth matter effect (panels 1, 3 and 5), as well as for SN neutrinos passing through earths mantle and core (panels 2, 4 and 6). We also plot the statistical error bands (1σ) assuming $\sqrt{N}$ errors. These plots show that the total number of charged current events can separate between different mass hierarchies (at 1σ) for $\tan^2\theta_{13} > 2.3\times10^{-5}$, 3.5×10^{-5}, 7.4×10^{-5} for the $\bar{\nu}_e + p$, $\bar{\nu}_e + ^{12}C$ and $\nu_e + ^{12}C$ reactions respectively for the case of no earth matter effect and for $\tan^2\theta_{13} > 2.9\times10^{-5}$, 4.4×10^{-5}, 3.4×10^{-5} for the case when we include earth matter effect. We notice that in the case of ν_e events, the difference between the number of events for NH and IH is enhanced with the introduction of earth matter effect if $\tan^2\theta_{13} \gtrsim$ a few times 10^{-5}. For neutrinos events with IH, $P_{ee}^{IH} \sim \sin^2\theta_{12} \sim 0.3$ (cf. figure 2) for the case of no earth effect whereas with earth effect it is $P_{ee}^{IH} \sim P_{2e}^{\oplus} \sim (f_{reg} + \sin^2\theta_{12})$. We have checked that the factor f_{reg} defined in Eq. (29) is mostly positive for all energies. This implies that P_{ee}^{IH} is higher for neutrinos crossing the earth so that there is less flavour conversion and hence from Eq. 31 we see that the number of events will be lower as seen in figure 4. For NH on the other hand, the earth regeneration effect is suppressed by the sharp fall of P_H with θ_{13} and one does not observe a pronounced change in the number of events due to earth effect in this range of $\tan^2\theta_{13}$. The net effect is an enhancement in the difference between the event rates for the two hierarchies in the case of ν_e events resulting in a better sensitivity towards separating between these. On the other hand, for $\bar{\nu}_e$ events, the difference between the hierarchies is seen to reduce for neutrinos crossing the earth.

To illustrate how the total number of events can be used to put bounds on θ_{13} and separate between the two hierarchies, we draw horizontal projections on the number of events axes from the points at which the slope of the rate-curve changes. This is shown in figure 4 by the horizontal lines marked by small English alphabets a, b, c, etc. Next we drop vertical projections on the $\tan^2\theta_{13}$ axis and find out the corresponding range of θ_{13}. The θ_{13} bounds are marked by the vertical projections A, B, C etc. In Table II we give the observed number of events between the different horizontal lines and the inferences on hierarchy and θ_{13} that one can draw from these observations for the three CC reactions. For purpose of illustration we give this Table for the case when the neutrinos are not passing through the earth. However similar conclusions can also be drawn for the case when the time of occurrence of the SN

Reactions	Range of observed events	conclusions drawn
$\bar{\nu}_e$+p→n+e$^+$	N< 485(a)	NH with no bound on θ_{13} OR IH with $\tan^2\theta_{13} < 2.3\times10^{-5}$(B)
	485(a)<N<501(b)	NH with $\tan^2\theta_{13} > 6.2\times10^{-3}$(G) OR IH with $\tan^2\theta_{13} < 3.4\times10^{-5}$(C)
	501(b)<N<530(c)	IH with $8.7\times10^{-6}(A) < \tan^2\theta_{13} < 4.7\times10^{-5}(D)$
	530(c)<N<615(d)	IH with $2.3\times10^{-5}(B) < \tan^2\theta_{13} < 2.9\times10^{-4}(F)$ OR IH with $\tan^2\theta_{13} > 8.4\times10^{-3}(H)$
	N>615(d)	IH with $\tan^2\theta_{13} > 8.6\times10^{-5}$(E)
$\bar{\nu}_e$+^{12}C→^{12}B+e$^+$	N< 29(a)	NH with no bound on θ_{13} OR IH with $\tan^2\theta_{13} < 3.3\times10^{-5}$(B)
	29(a)<N<33(b)	NH with $\tan^2\theta_{13} > 5.6\times10^{-3}$(G) OR IH with $\tan^2\theta_{13} < 4.9\times10^{-5}$(C)
	33(b)<N<41(c)	IH with $6.8\times10^{-6}(A) < \tan^2\theta_{13} < 1.4\times10^{-4}(D)$
	41(c)<N<44(d)	IH with $3.3\times10^{-5}(B) < \tan^2\theta_{13} < 2.3\times10^{-4}(F)$ OR IH with $\tan^2\theta_{13} > 1.2\times10^{-2}(H)$
	N>44(d)	IH with $\tan^2\theta_{13} > 4.2\times10^{-5}$(E)
ν_e+^{12}C→^{12}N+e$^+$	N< 63(a)	IH with no bound on θ_{13} OR NH with $\tan^2\theta_{13} < 7.4\times10^{-5}$(B)
	63(a)<N<66(b)	IH with $\tan^2\theta_{13} > 1.0\times10^{-2}$(G) OR NH with $\tan^2\theta_{13} < 1.1\times10^{-4}$(C)
	66(b)<N<70(c)	NH with $7.8\times10^{-6}(A_2) < \tan^2\theta_{13} < 2.5\times10^{-4}(F)$ OR NH with $\tan^2\theta_{13} > 1.3\times10^{-2}(H)$
	N>70(c)	NH with $\tan^2\theta_{13} > 2.5\times10^{-4}$(E)

TABLE II: The inferences on hierarchy and allowed range of θ_{13} that can be drawn from figure 4 from the observation of total number of events. We present the inferences for the panels 1,3 and 5 in figure 4. a, b, c, d, e correspond to the points shown in figure 4. The bounds on θ_{13} correspond to vertical projections from a, b, c, d, e on the θ_{13} axis from the points where the horizontal lines meet the rate-curves.

makes the neutrinos traverse through the earth. We see from the Table that if we consider one particular reaction then the number of events lying between the different horizontal lines can:
(1) identify the hierarchy uniquely and indicate the θ_{13} range,
(2) allow both hierarchies and put some bound on θ_{13} for either or both of these.
In the case when a unique solution is not obtained from one reaction it may help to take recourse to a second reaction channel. For instance considering the $\bar{\nu}_e + p$ reaction we find from Table II that if the total event rate, $N < 485$ then there are two possibilities:
(i) the hierarchy is normal and no bound can be put on θ_{13},
(ii) the hierarchy is inverted and $\tan^2\theta_{13} \lesssim 2.3\times10^{-3}$.
The ambiguity in hierarchy can however be resolved if in the $\nu_e + ^{12} C$ reaction one observes $N > 66$. For this case one can definitely say that the hierarchy is normal and obtain a lower bound of $\tan^2\theta_{13} > 7.8\times10^{-6}$. With the identification of the hierarchy as normal, the lower bound can be improved to $\tan^2\theta_{13} > 5.6\times10^{-6}$ if in the $\bar{\nu}_e + ^{12} C$ reaction one observes $29 - 33$ events. Even when the number of events observed in one particular reaction gives a unique solution for the hierarchy and the allowed range of θ_{13}, it may be possible to use the observed number of events in another reaction effectively to further constrain the allowed θ_{13} range.

We would like to point out here that this is an exploratory analysis which studies the sensitivity of the total number of events to θ_{13} and the mass hierarchy. The exact values of the bounds quoted in Table II are not so important. An appropriate χ^2 analysis procedure including all the uncertainties and parameter correlations will allow to study the conclusions obtained in more detail and with a greater statistical significance.

energy bins in MeV	Minimum detector volume (in kiloton) required for different reactions		
	$\bar{\nu}_e + p$	$\bar{\nu}_e + ^{12}C$ CC	$\nu_e + ^{12}C$ CC
21-26	very large	very large	8
26-31	29	very large	11
31-36	51	5	78
36-41	10	88	very large
41-46	2	9	5

TABLE III: Minimum volume required for a scintillator detector to statistically distinguish the number of events between two scenarios: neutrinos undergoing no earth matter effects and neutrinos passing through earth's core and mantle.

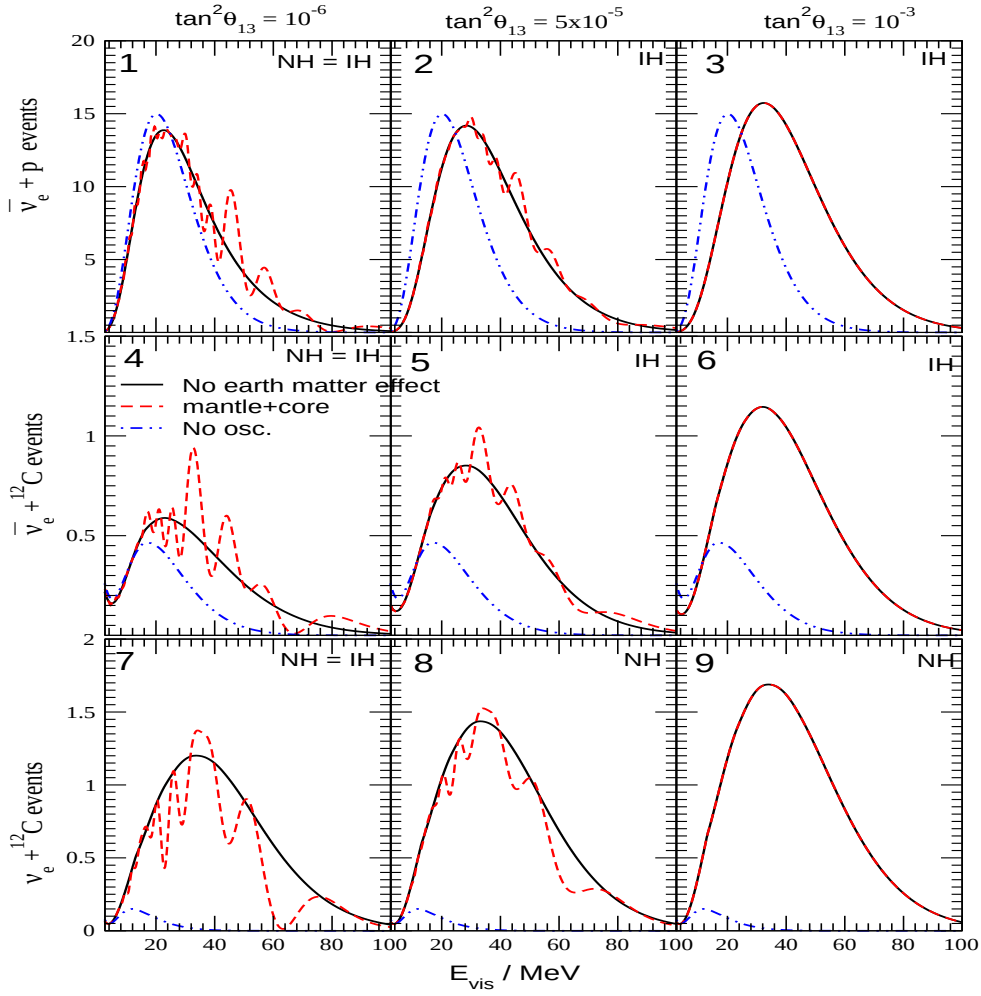

FIG. 5: The CC spectra due to $\bar{\nu}_e + p$, $\bar{\nu}_e + ^{12}C$ and $\nu_e + ^{12}C$ events in KamLAND. The solid curves are for the case with no earth matter effect and the dashed curves are for the case when the neutrinos pass through earths mantle and core. The dotted lines correspond to the unoscillated spectrum. We plot the spectrum for three sample values of θ_{13}. For the $\bar{\nu}_e(\nu_e)$ events the spectra for NH(IH) are identical to the one presented for $\tan^2\theta_{13} = 10^{-6}$ and hence these are not drawn for the higher θ_{13} values.

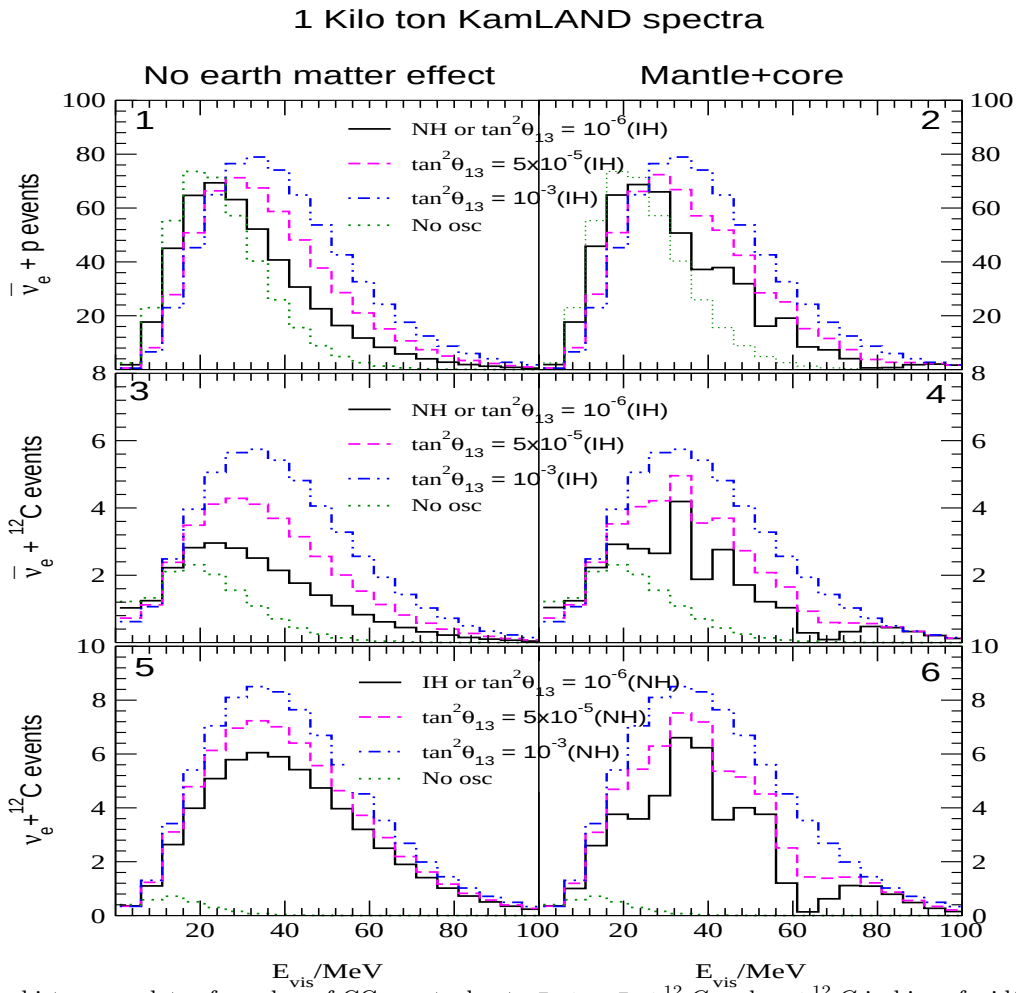

FIG. 6: Energy histogram plots of number of CC events due to $\bar{\nu}_e + p$, $\bar{\nu}_e + ^{12} C$ and $\nu_e + ^{12} C$ in bins of width 5 MeV for the KamLAND detector.

B. Using the charged current spectrum

For the CC absorption of $\bar{\nu}_e$ on free protons and $\bar{\nu}_e$ and ν_e reactions on ^{12}C, the detectors can observe the distribution of the event rates with energy of the emitted electron or positron. As the average energies of the $\nu_\mu/\nu_\tau(\bar{\nu}_\mu/\bar{\nu}_\tau)$ are greater than the average energy of $\nu_e(\bar{\nu}_e)$, the oscillated $\nu_e(\bar{\nu}_e)$ will have a harder spectrum. This hardening of the energy spectrum of the neutrinos is manifested in the observed positron/electron events in the detector, since one has more high energy events compared to what would be expected in absence of oscillations. In addition, if the neutrino survival probabilities are energy dependent, then this would introduce a further distortion in the shape of the resultant spectrum. There are two possible sources of energy dependence in the survival probabilities:
(i) matter effect in the supernova – this inducts an energy dependence in $P_{\bar{e}\bar{e}}^{IH}$ and P_{ee}^{NH} through P_H, in the intermediate θ_{13} range;
(ii)matter effect inside the earth – this leads to Δm^2_{21} driven energy dependent frequency modulations.

In figure 5 we show the un-binned positron/electron spectrum for the (*i*) $\bar{\nu}_e + p$, (*ii*) $\bar{\nu}_e + ^{12} C$ and (*iii*) $\nu_e + ^{12} C$ reactions in KamLAND. The dot-dashed curve gives the spectra for the case of no oscillation, the solid curves are for the case where we have oscillation inside the SN but with no earth matter effects, while the dashed curves show the spectrum expected when the supernova neutrinos cross the earth's mantle and core. For the case where $\tan^2\theta_{13} = 10^{-6}$, the CC spectra for both ν_e and $\bar{\nu}_e$ channel are identical for IH and NH (panels 1,4 and 7). For $\bar{\nu}_e(\nu_e)$ flux with NH(IH) as the true hierarchy, the event spectra are not expected to change with θ_{13} in the range limited by the CHOOZ constraints. Therefore we present the $\bar{\nu}_e(\nu_e)$ spectra for NH(IH) only in the panels 1, 4 and 7. On the other hand the $\bar{\nu}_e(\nu_e)$ spectra for IH(NH) will depend on the value of θ_{13} both for with and without earth matter effects. In the remaining panels we show the spectra for these cases for two different values of $\tan^2\theta_{13} - 5 \times 10^{-5}$ and

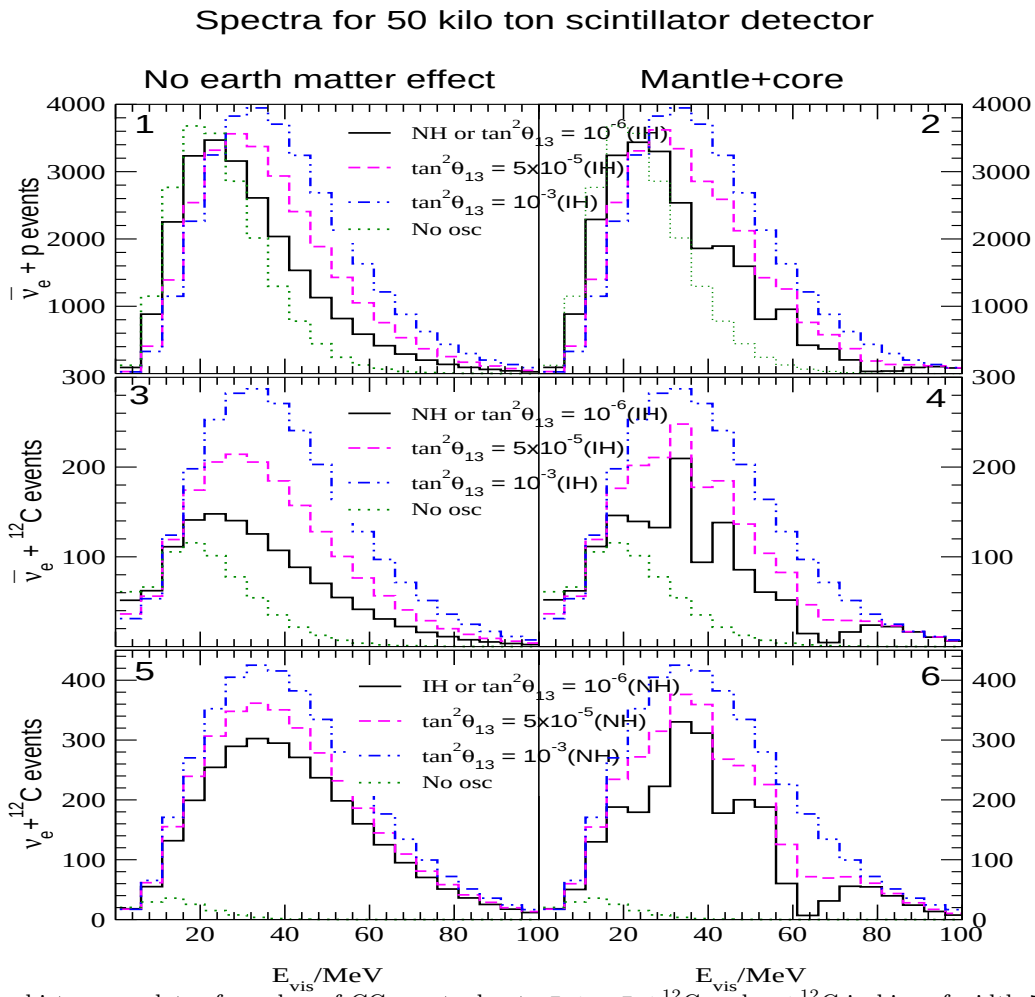

FIG. 7: Energy histogram plots of number of CC events due to $\bar{\nu}_e$+p, $\bar{\nu}_e$+^{12}C and ν_e+^{12}C in bins of width 5 MeV for a 50 kilo ton scintillator detector like LENA.

10^{-3}. We also note from this figure the fast variation of the spectrum shape due to earth matter effects.

In figure 6 we show the expected energy spectrum for the three possible CC reactions in KamLAND in bins of 5 MeV width. The left-hand panels show the expected spectra without earth matter effect while the right-hand panels display what we expect in case the neutrino cross the earth. For both the $\bar{\nu}_e$ and ν_e events, the solid curve denotes the case of $\tan^2\theta_{13} = 10^{-6}$ and it corresponds to both NH and IH. For $\bar{\nu}_e(\nu_e)$ events with NH(IH) the spectra remains the same as that shown by the solid lines for all values of θ_{13}, however for IH(NH) the spectra will change with θ_{13}. These are shown by the dashed and dot-dashed lines for two different values of $\tan^2\theta_{13}$. The dotted lines show the no-oscillation spectra.

1. *No earth matter effect*

The comparison of the curves corresponding to the case of no oscillation in figures 5 and 6 to the ones with oscillations, show the effect of oscillations in general on the expected spectrum in KamLAND.

For a given hierarchy, say IH for $\bar{\nu}_e$ (panels 1 and 3 of figure 6) or NH for ν_e (panel 5 of figure 6), if we compare the spectra for different values of $\tan^2\theta_{13}$, we note an increase in the number of events in higher energy bins, with the increase in the value of $\tan^2\theta_{13}$. This is due to the change in the relevant survival probability due to matter effect in the SN. For $\tan^2\theta_{13} \sim 10^{-6}$, $P_H = 1$ and we have only the lower resonant conversion in the SN. As $\tan^2\theta_{13}$ increases, P_H decreases and eventually becomes zero at $\tan^2\theta_{13} \sim 10^{-3}$. A small P_H implies a lower survival probability, more flavor conversion and hence harder spectrum for the incoming (anti)neutrinos. This change in the shape of the spectrum with θ_{13} can be used to limit the value of $\tan^2\theta_{13}$ for a given hierarchy. Also, since for NH(IH), the

$\bar{\nu}_e(\nu_e)$ spectrum are independent of $\tan^2\theta_{13}$ and correspond to the the curves shown by bold solid lines in figure 6, a comparison of the observed spectrum against the expected ones can shed some light on the neutrino mass hierarchy, if true value of $\tan^2\theta_{13}$ is $\gtrsim 10^{-6}$. Note however that the value of $\tan^2\theta_{13}$ and the neutrino mass hierarchy come correlated. For instance, if the observed spectrum corresponds to the one shown by the solid black line in panel 1 of figure 6 for $\bar{\nu}_e + p$ events, then it would be difficult to decide whether the hierarchy is inverted and $\tan^2\theta_{13} \lesssim 10^{-6}$ or the hierarchy is normal with no bound on θ_{13}, using only this reaction. However, if in addition the observed spectral shape corresponding to electron events generated by the $\nu_e + ^{12} C$ reaction conforms to the one shown by, say, the dot-dashed line in panel 5 of figure 6, then we can say that the mass hierarchy is normal and one can put a lower bound on $\tan^2\theta_{13}$.

2. Including earth matter effect

Matter effects inside the earth produce Δm^2_{21} driven oscillations [18, 20, 25, 27, 28] which we see in the dashed curves shown in figure 5 and right-hand panels in figure 6. These high frequency oscillations in the energy spectrum are superimposed over the dominant spectral distortion due to transitions in the supernova. Observation of these fast modulations in the observed spectrum would give an unambiguous signature of the presence of earth effects, which can be used to constrain the hierarchy and θ_{13}. In particular, we note that there are no earth induced wiggles in the resultant $\bar{\nu}_e(\nu_e)$ spectrum for $\tan^2\theta_{13} \gtrsim 10^{-3}$ for IH(NH). However, if the hierarchy is normal(inverted) then even if $\tan^2\theta_{13} \gtrsim 10^{-3}$, one would expect earth matter effects in the $\bar{\nu}_e(\nu_e)$ spectrum as is evident from panels 1, 4 and 7 of figure 5 and the solid black lines in figure 6, which show the spectra for these cases. Thus the detection of earth matter effects in the antineutrino(neutrino) channel for $\tan^2\theta_{13} \gtrsim 10^{-3}$ would clearly indicate normal(inverted) hierarchy for the neutrino mass spectrum. If we use the earth matter signatures from just the neutrino or the antineutrino channel alone, we would need some prior information that $\tan^2\theta_{13} \gtrsim 10^{-3}$. This could come either from the total rates signature of the supernova signal itself (as discussed in the previous sub-section) or from some other terrestrial experiment. However, if we use the neutrino and antineutrino channel simultaneously and look for earth matter effects, we could pin down both the neutrino mass hierarchy and the range of $\tan^2\theta_{13} \gtrsim 10^{-3}$, if this indeed was the true range of $\tan^2\theta_{13}$. For example, if we observe no earth matter dependent modulations in the neutrino channel and at the same time observe the earth matter generated wiggles in the antineutrino channel, we could surely say that the hierarchy is normal and $\tan^2\theta_{13} \gtrsim 10^{-3}$.

3. Detection of earth matter effect induced modulations

The figure 5 reflects the fact that the earth effect induced modulations are more rapid but of less amplitude in the low energy regime, whereas in the high energy domain they are less rapid but of greater amplitude. Since in the low energy regime the modulations are very frequent in energy, they are averaged out even in a very narrow energy bin. So it is not possible for any detector to observe the "earth matter effect induced modulations" in the lower energy bins (cf. figure 6). On the other hand, towards the higher energy regime, the modulations are highly peaked and more wide (roughly the same order as the width of the energy bins we take), and hence may be observed in the event distribution, as can be seen in figure 6. If the energy resolution is poor which means a measured electron/positron energy corresponds to a wide range of true energy (and hence neutrino energy) then even the wide modulations at high energy domain may be averaged out within this range and consequently these modulations can't be seen even in the higher energy bins. So a detector needs a very good energy resolution to detect the earth matter effect induced modulations. KamLAND being a scintillation detector fulfills this criterion very well and we note from the right-hand panels of figure 6 that KamLAND does see the earth induced modulations in the energy spectrum at the high energy end. However, even though the event rate in KamLAND for the $\bar{\nu}_e + p$ reaction is not very low, the statistics in KamLAND in the individual spectral bins for the ^{12}C reactions are poor with the present volume of 1 kton. This could therefore preclude any statistically significant signature for earth matter effects in KamLAND at least in the ^{12}C reaction channels. We therefore need larger KamLAND like scintillation detectors for observing the earth matter effects in the detected supernova spectrum, where these ^{12}C reactions could be probed to look for earth matter effects. In Table III we give the minimum detector mass required for a KamLAND type scintillator detector to observe statistically significant earth matter effect induced wiggles in various energy bins. The Table III shows that in general we need lower detector mass to detect the modulations in the higher energy bins. For the lower energy bins (which have a better statistics) the $\nu_e + ^{12} C$ reaction is most promising and can detect the earth matter effect modulations with a much smaller volume detector.

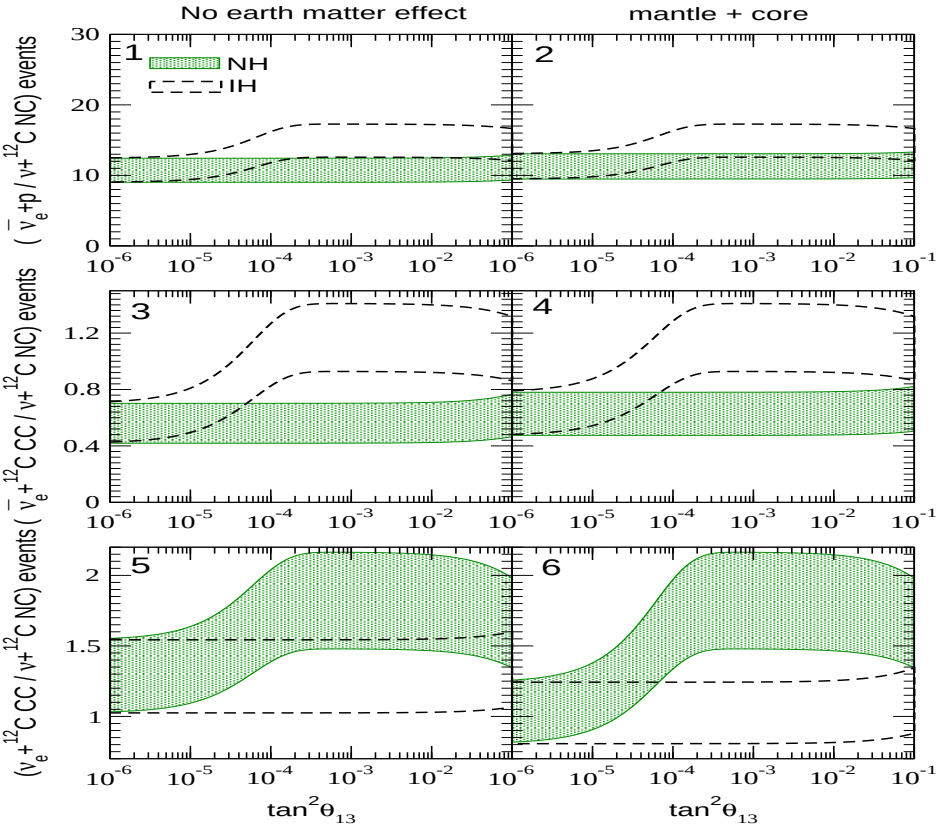

FIG. 8: Plot of ratio of $\nu_e(\bar{\nu}_e)+ {}^{12}C$ CC event rates to $(\nu+{}^{12}C)$ NC event rates as a function of θ_{13} for NH and IH, including the statistical uncertainty

4. The CC spectrum for a 50 kton detector

Even though from figure 6 we see that the statistics for the $\bar{\nu}_e + p$ reaction is not very poor in KamLAND, this reaction feels lesser impact of the earth generated modulations of the spectrum in the energy bins near the peak. On the other hand the ^{12}C reactions have greater fluctuations over the no earth effect spectra in the energy bins near the peak. Thus the ^{12}C reactions seem to have a better potential to probe earth effects in the resultant spectrum. But one needs a larger detector to study the energy spectra of these reactions and make a statistically significant statement. In figure 7 we show the corresponding expected energy binned spectrum in a 50 kton liquid scintillation detector. Recently a large liquid scintillation detector, LENA, has been proposed which would have a total mass of 50 kton and a fiducial mass of about 30 kton [54]. We use the largest possible detector mass for the sake of illustration. This figure is a "scaled up" version of figure 6 and all the features discussed in the context of figure 6 appear in a much magnified form here. In particular, the fast oscillations imprinted on the spectra ^{12}C corresponding to $\bar{\nu}_e$ and ν_e reactions can be combined to lead to unambiguous determination of the hierarchy and limit on the value of θ_{13}, as discussed before for KamLAND. For LENA it can be verified with a good statistical precision. The $\bar{\nu}_e + p$ process in LENA would have a statistics comparable to that expected in SK – with much better energy resolution and hence greater spectral power.

VI. SN UNCERTAINTIES AND CC/NC RATIOS

In the previous sections we have considered the effect of statistical errors only. However there are uncertainties emerging from our (lack of) knowledge of neutrino fluxes in a supernova due to:
• uncertainty in the total value of neutrino luminosity

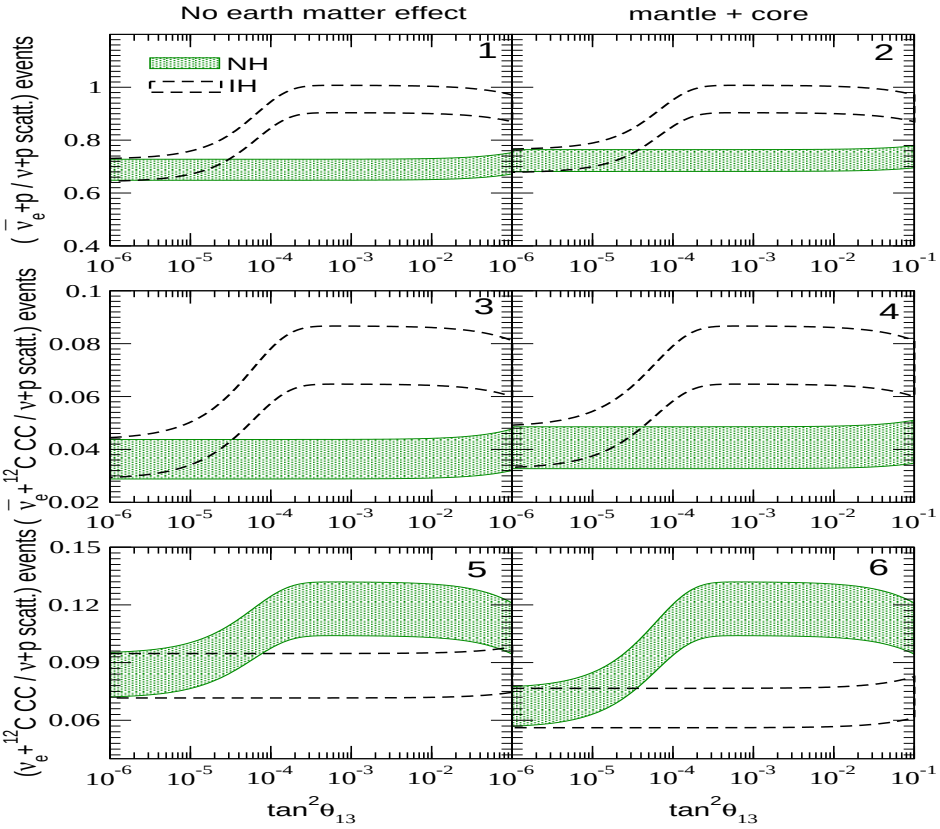

FIG. 9: Plot of ratio of $\nu_e(\bar{\nu}_e) + {}^{12}C$ CC event rates to $(\nu + p)$ scattering event rates as a function of θ_{13} for NH and IH, with the statistical uncertainty.

• uncertainty in the luminosity distribution between the 6 species
• uncertainty in the average temperature of each neutrino species
• uncertainty in the value of pinching factor in the neutrino spectra which leads to deviation from the Fermi-Dirac distribution

In our calculation so far we have used $L_e = L_{\bar{e}} = L_x = L_{\bar{x}}$ where x can be μ or τ. However these can vary as $L_{e/\bar{e}} = (0.5 - 2)L_{x/\bar{x}}$ with L_x and $L_{\bar{x}}$ being equal [37]. The average energies of ν_e, $\bar{\nu}_e$ and ν_x can vary in the range $(7 - 18)$ MeV, $(14 - 22)$ MeV and $(15 - 35)$ MeV [37]. The pinching factor can take values between $(0 - 2)$ for ν_x and $(0 - 3)$ for ν_e and $\bar{\nu}_e$. Finally the absolute luminosity can be uncertain in the range $(1 - 5) \times 10^{52}$ ergs. Incorporation of these uncertainties can change the above conclusions. These uncertainties are correlated and a proper treatment requires a χ^2 analysis incorporating these uncertainties in a correlated fashion. In this section we explore if it is possible to construct variables which are free from some of the uncertainties and introduce the CC/NC ratios. We study the capability of these ratios in separating between the normal and inverted hierarchies and also their sensitivity to θ_{13}. These ratios have the advantage that the uncertainty due to the total luminosity gets canceled out from the numerator and the denominator.

As we have discussed in section 4, KamLAND is sensitive to two NC reactions (i) $\nu + {}^{12}C$ and (ii) $\nu + p$. In figure figure 8 we plot the CC/NC ratios as a function of θ_{13}, for normal and inverted hierarchy with 1σ statistical error bands. The NC reaction considered is the $\nu + {}^{12}C$ reaction. In figure 9 we plot the same thing but using the $\nu - p$ scattering reaction as the NC reaction channel.

It is instructive to look at the %-spread in the widths of the error bands relative to the central value for each case as well as for the CC rates in figure 4. The % spread is defined as

$$\text{spread} = \frac{R_{upper} - R_{lower}}{\text{R}_{\text{central}}} \times 100 \tag{43}$$

where R denotes the values of the event rates or ratios at the appropriate limit denoted by the suffix. When we take

Reactions	CC events	CC/$\nu + ^{12}C$ NC events	CC/ν+p scatt. events
$\bar{\nu}_e + p$	3.94(4.66)	15.72(15.92)	5.51(6.04)
$\bar{\nu}_e + ^{12}C$	14.11(20.31)	20.75(25.38)	16.22(22.94)
$\nu_e + ^{12}C$	13.42(11.12)	20.39(18.90)	14.33(11.96)

TABLE IV: The 1σ % spreads defined in Eq. (43) at $\tan^2\theta_{13} = 10^{-3}$ for IH(NH).

Reactions	CC events	CC/$\nu + ^{12}C$ NC events	CC/$\nu + p$ scatt. events
$\bar{\nu}_e + p$	11.81	0	10.51
$\bar{\nu}_e + ^{12}C$	19.06	13.32	18.91
$\nu_e + ^{12}C$	4.73	-1.63	4.50

TABLE V: The "separation" as defined in Eq. (44) for different CC events as well as for the CC/NC ratios. The separations in this Table are calculated at a sample value of $\tan^2\theta_{13} = 10^{-3}$.

the ratio of CC event rates(x) to the NC event rate(y), the % spread is $\sqrt{(1/x + 1/y)}$. Therefore larger the NC event rate smaller is the spread and so the $\nu - p$ reactions are expected to have smaller spread than the $\nu - ^{12}C$ reaction. It is relevant to point out here that the % spread for the the CC rates goes as $\sqrt{(1/x)}$ and hence it will have a narrower % spread as far as statistical error is concerned. In Table IV we show the % spreads for $\tan^2\theta_{13} = 10^{-3}$ for the three reactions. The Table shows that the % spread is least for the CC rates. However the effect of the absolute luminosity uncertainty (from which the ratios are free) may offset this advantage for the CC rates.

When we study the effectiveness with which one can separate between normal and inverted hierarchies it is useful to define the quantity

$$\text{separation} = 100 \times \left(\frac{\mathrm{R}^{\mathrm{H}_1}_{\mathrm{lower}} - \mathrm{R}^{\mathrm{H}_2}_{\mathrm{upper}}}{\mathrm{R}^{\mathrm{IH}}_{\mathrm{central}} + \mathrm{R}^{\mathrm{NH}}_{\mathrm{central}}} \right) \tag{44}$$

where for $\bar{\nu}_e(\nu_e)$ events the suffixes H_1 and H_2 in the first and the second term in the numerator will correspond to IH(NH) and NH(IH) respectively. The suffix "central" denote the the central values of event rates or ratios. The subscripts "upper" and "lower" are used to indicate respectively the (central + 1σ) and (central - 1σ) values.

In Table V we show this quantity for the CC rates as well as for the ratios for purposes of illustration for the specific case of $\tan^2\theta_{13} = 10^{-3}$ and with no earth matter effect. It is clear from the table that at least at this value of θ_{13}, the CC/NC ratios w.r.t the $\nu - p$ NC scattering does an even better job than the CC rates, with the added advantage that the ratios are free from the uncertainties due to absolute luminosity. From figures 9 (and also figure 4) we can convince ourselves that this conclusion is valid for other values of θ_{13} as well, if θ_{13} is not too small, for which in any case the SN neutrinos loose the sensitivity to separate between the hierarchies. As we have seen earlier with the introduction of earth matter effect for the ν_e events there is more earth regeneration for IH implying there is less conversion and the number of events for IH decreases and hence the difference between IH and NH increases (cf. fig. 2) as compared to the no earth matter effect case. Thus when neutrinos pass through earth, the ν_e events gain a better capability of distinguishing between the hierarchies.

The Table V and the figure 8 show that when the ratio is taken w.r.t the $\nu - ^{12}C$ reaction the potential of the the CC/NC variable to distinguish between normal and inverted hierarchies worsens for the $\bar{\nu}_e + p$ and the $\nu_e + ^{12}C$ reaction and the NH and IH becomes indistinguishable excepting the case of panel 6 in figure 8 for the $\nu_e + ^{12}C$ reaction where earth matter effect helps.

VII. SUMMARY AND CONCLUSIONS

Although the neutrino fluxes from supernova suffer from inherent astrophysical uncertainties which can be large, the physics potential offered by them are quite rich. A core-collapse supernova provides an unique environment where one can study the propagation and matter effect of all three species of neutrinos and antineutrinos. The varying density in supernova allows the occurrence of two MSW resonances corresponding to both atmospheric and solar mass scale and if a detector is placed such that the neutrinos from the supernova traverse through the earth's mantle and/or core then earth matter effects also come into play.

As far as the propagation in SN matter is concerned, the solar neutrino oscillation parameters lying in the LMA region govern the lower resonance and the propagation is fully adiabatic. Propagation through the higher resonance could be non-adiabatic depending on the hierarchy and θ_{13}. For $\bar{\nu}_e(\nu_e)$ with IH(NH) there are three possibilities determined by the mixing angle θ_{13}:
(i) If $\tan^2\theta_{13} \lesssim 10^{-6}$, the propagation at higher resonance is completely non-adiabatic, $P_H = 1$, and the survival probability is identical for IH and NH for both ν_e and $\bar{\nu}_e$. In this regime it is not possible to differentiate between NH and IH and only an upper limit on θ_{13} can be given.
(ii) For $10^{-6} \lesssim \tan^2\theta_{13} \lesssim 10^{-3}$, the propagation is partially non-adiabatic for neutrinos (antineutrinos) and normal(inverted) hierarchy and depends on P_H. P_H changes from 1 to 0 depending on the value of θ_{13} and one can constrain θ_{13} within a range.
(iii) For $\tan^2\theta_{13} \gtrsim 10^{-3}$ the propagation is completely adiabatic($P_H = 0$) for the $\nu_e(\bar{\nu}_e)$ and normal(inverted) hierarchy and flavour conversion is maximum. The probabilities do not vary with θ_{13} in the range permitted by the CHOOZ data. In this regime one can therefore set only a lower bound on θ_{13}.
(iv) The $\nu_e(\bar{\nu}_e)$ propagation in SN matter for inverted(normal) hierarchy have no dependence on P_H and the survival probabilities do not change with θ_{13}. Therefore if θ_{13} is such that the value of P_H is expected to be different from 1 for $\nu_e(\bar{\nu}_e)$ and normal(inverted) then observation of total number of events can distinguish between the hierarchies in both neutrino and antineutrino channel. The power of discrimination between the two hierarchies is maximum in the region (iii) above where P_H differs maximally from 1.

This dependence of the probabilities on θ_{13} and hierarchy gives SN neutrinos (at least in principle) remarkable sensitivity to probe very small values of θ_{13}, much smaller than the projected limits from the reactor experiments, superbeams and even neutrino factories, and also the mass hierarchy.

We study in detail the sensitivity of the the total observed event rates, in the $\bar{\nu}_e + p$, $\bar{\nu}_e + {}^{12}C$ and $\nu_e + {}^{12}C$ reactions in the KamLAND detector to probe θ_{13} and to distinguish between normal and inverted hierarchy. We find that considering only the statistical errors into account, it may be possible to uniquely determine the hierarchy and give a bound on the allowed range of θ_{13}. In some cases it may not be possible to disentangle the correlated information on hierarchy and the allowed range of θ_{13} from the observation of total number of events in one reaction channel. However a distinction may be possible using the observed event rates in another reaction. We find that it is particularly useful to combine the information from $\bar{\nu}_e$ and ν_e reaction channels.

Apart from the total event rates it is also possible to observe the CC spectrum due to (i) $\bar{\nu}_e + p$, (ii) $\bar{\nu}_e + {}^{12}C$ and (iii) $\nu_e + {}^{12}C$ reactions in KamLAND. Since the average energies of muon and tau type neutrinos are more, the flavor converted electron type neutrinos and antineutrinos will have a harder spectrum even if the probabilities are energy independent. The matter effect in the SN may induce an additional energy dependence in the probabilities P_{ee}^{NH} and $\mathrm{P}_{\bar{e}\bar{e}}^{IH}$ if θ_{13} lies in the intermediate range. As θ_{13} increases there is more flavor conversion giving rise to more neutrinos in the higher energy bins. This hardening of the spectrum can be used to put bounds on θ_{13}. On the other hand ν_e events for IH and $\bar{\nu}_e$ events for NH do not display this extra θ_{13} dependent hardening of the spectrum. This can therefore be used to separate between the hierarchies.

If in addition there is earth matter effect then it gives rise to fast modulations of the event rate with energy. For the $\bar{\nu}_e(\nu_e)$ spectra, while these modulations are independent of θ_{13} for NH(IH), for IH(NH) they are decrease with the rise of θ_{13} and vanish for $\tan^2\theta_{13} \gtrsim 10^{-3}$. Therefore observation of these earth effect induced modulations give a handle to probe θ_{13} and the true mass hierarchy.

To observe this modulations one needs a very good energy resolution and KamLAND being a scintillator detector is ideal for the purpose. We also study the potential of the capture reactions of ν_e and $\bar{\nu}_e$ on ${}^{12}C$, for observing the earth matter induced fast fluctuations in the observed spectrum. However these reactions have low statistics in KamLAND which has only 1 kton of detector mass. We determine the minimum volume that is required to observe the modulations due to earth matter effect in a generic scintillation detector in various energy bins. We present for a planned 50 kton detector the energy spectrum for various values of θ_{13} and discuss how the energy spectrum can be used to differentiate between θ_{13} and also to discriminate between the hierarchies.

We also construct the CC/NC ratios which are better as far as the SN uncertainties are concerned, since the absolute uncertainties can get canceled in these ratios. However since the ratios have a larger relative statistical error their usefulness is limited unless the statistics of the NC events are very large. The two NC reactions that the SN neutrinos can undergo in KamLAND are $\nu - {}^{12}C$ and $\nu - p$ reaction. Since the latter has a far better statistics, it is superior to the $\nu - {}^{12}C$ reaction for probing θ_{13} and hierarchy. We find that the CC/NC ratio w.r.t the $\nu - p$ scattering reaction even has a better power to separate between the hierarchies compared to the only CC rates.

To conclude, in this paper we have made an in-depth study of the potential of the KamLAND detector in probing θ_{13} and sign of the atmospheric mass scale Δm^2_{32} through observation of SN neutrinos. The results look promising and warrants a more rigorous statistical analysis simulating the supernova signal and including the astrophysical uncertainties with their proper correlation.

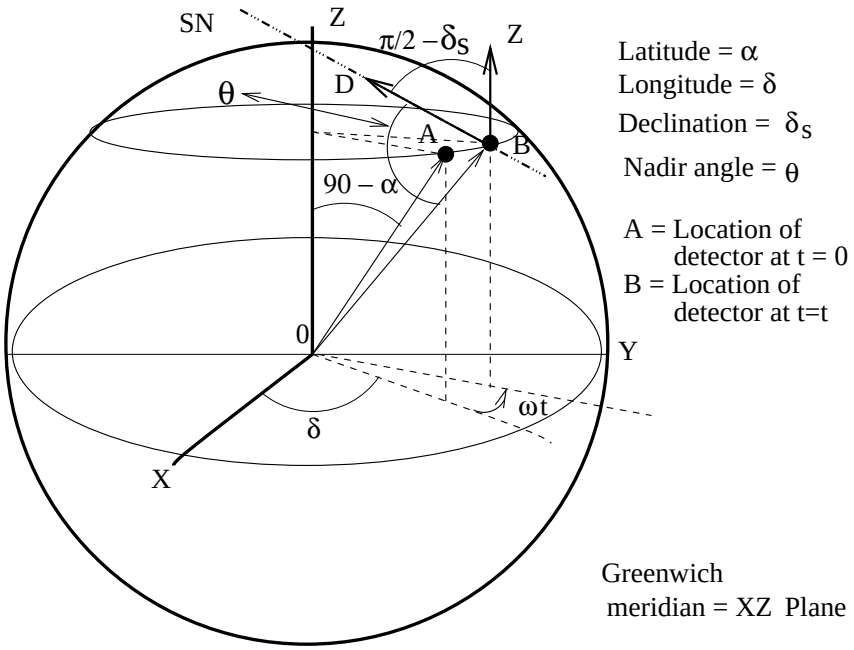

FIG. 10: The geometry describing the trajectory of a neutrino from supernova inside the earth in reaching a detector.

Appendix A

For a given location of the supernova the nadir angle subtended at a particular detector also changes continually with time as the earth precesses about it axis of rotation with an angular speed of $\frac{2\pi}{24}$ hours^{-1}. The figure 10 describes this geometry. The direction of the supernova from earth can be specified by the angle δ_s (the declination), which is the angle that the supernova direction makes with the plane of the equator. We denote the latitude and longitude of the detector by (α,δ) and the angular speed of earth's rotation about its own axis by ω. We define an universal time which is counted from a moment (t=0) when the supernova is on the Greenwitch meridian.Then one can write the nadir angle θ_n of the detector at time t as

$$\cos\theta_n \;=\; -(\cos\alpha\cos\delta_s\cos(\omega t+\delta)+\sin\alpha\sin\delta_s) \tag{45}$$

For $\cos\theta_n < 0$ the SN neutrinos do not cross the earth, for $0 < \cos\theta_n < 0.84$ the neutrinos pass through the earth's mantle, while for $0.84 < \cos\theta_n < 1$ they pass through both the mantle and core of the earth.

S.G. would like to thank Mark Vagins for useful correspondences. S.C. acknowledges discussions with Lothar Oberauer on the proposed LENA detector.

[1] K. Eguchi *et al.* [KamLAND Collaboration], Phys. Rev. Lett. **90**, 021802 (2003) [arXiv:hep-ex/0212021].
[2] L. Wolfenstein, Phys. Rev. D **17**, 2369 (1978) ; S. P. Mikheev and A. Y. Smirnov, Sov. J. Nucl. Phys. **42** (1985) 913 [Yad. Fiz. **42**, 1441 (1985)] ; S. P. Mikheev and A. Y. Smirnov, Sov. J. Nucl. Phys. **42** (1985) 913 [Yad. Fiz. **42**, 1441 (1985)]
[3] B. T. Cleveland *et al.*, Astrophys. J. **496**, 505 (1998); J. N. Abdurashitov *et al.* [SAGE Collaboration], arXiv:astro-ph/0204245; W. Hampel *et al.* [GALLEX Collaboration], Phys. Lett. B **447**, 127 (1999); E. Bellotti, Talk at Gran Sasso National Laboratories, Italy, May 17, 2002; T. Kirsten, talk at *Neutrino 2002*, XXth International Conference on Neutrino Physics and Astrophysics, Munich, Germany, May 25-30, 2002. *(http://neutrino2002.ph.tum.de/).*
[4] S. Fukuda *et al.* [Super-Kamiokande Collaboration], Phys. Lett. B **539**, 179 (2002) [arXiv:hep-ex/0205075].
[5] Q. R. Ahmad *et al.* [SNO Collaboration], Phys. Rev. Lett. **87**, 071301 (2001) [arXiv:nucl-ex/0106015].
[6] Q. R. Ahmad *et al.* [SNO Collaboration], Phys. Rev. Lett. **89**, 011301 (2002) [arXiv:nucl-ex/0204008]. Q. R. Ahmad *et al.* [SNO Collaboration], on neutrino mixing parameters," Phys. Rev. Lett. **89**, 011302 (2002) [arXiv:nucl-ex/0204009];
[7] S. N. Ahmed *et al.* [SNO Collaboration], arXiv:nucl-ex/0309004.

[8] A. B. Balantekin and H. Yuksel, arXiv:hep-ph/0309079; G. L. Fogli, E. Lisi, A. Marrone and A. Palazzo, arXiv:hep-ph/0309100; M. Maltoni, T. Schwetz, M. A. Tortola and J. W. F. Valle, arXiv:hep-ph/0309130; A. Bandyopadhyay, S. Choubey, S. Goswami, S. T. Petcov and D. P. Roy, arXiv:hep-ph/0309174; P. C. de Holanda and A. Y. Smirnov, arXiv:hep-ph/0309299.

[9] A. Bandyopadhyay, S. Choubey, S. Goswami and D. P. Roy, Phys. Lett. B **540**, 14 (2002) [arXiv:hep-ph/0204286]. S. Choubey, A. Bandyopadhyay, S. Goswami and D. P. Roy, arXiv:hep-ph/0209222. and references therein.

[10] A. Bandyopadhyay, S. Choubey, S. Goswami and K. Kar, Phys. Lett. B **519**, 83 (2001) [arXiv:hep-ph/0106264].

[11] Super-Kamiokande Coll., Y. Hayato *et al.*, Talk given at the Int. EPS Conference on High Energy Physics, July 17 - 23, 2003, Aachen, Germany.

[12] M. Apollonio *et al.*, *Phys. Lett.* **B466** (1999) 415; F. Boehm *et al.*, *Phys. Rev.* **D62** (2000) 072002.

[13] Y. Itow *et al.*, arXiv:hep-ex/0106019.

[14] D. Ayres *et al.*, arXiv:hep-ex/0210005.

[15] H. Minakata, H. Sugiyama, O. Yasuda, K. Inoue and F. Suekane, Phys. Rev. D **68**, 033017 (2003) [arXiv:hep-ph/0211111].

[16] P. Huber, M. Lindner, T. Schwetz and W. Winter, Nucl. Phys. B **665**, 487 (2003) [arXiv:hep-ph/0303232].

[17] S. T. Petcov and M. Piai, Phys. Lett. B **533**, 94 (2002) [arXiv:hep-ph/0112074]; S. Choubey, S. T. Petcov and M. Piai, Phys. Rev. D (in press), arXiv:hep-ph/0306017.

[18] A. S. Dighe and A. Y. Smirnov, Phys. Rev. D **62**, 033007 (2000) [arXiv:hep-ph/9907423].

[19] K. Takahashi, M. Watanabe, K. Sato and T. Totani, Phys. Rev. D **64**, 093004 (2001) [arXiv:hep-ph/0105204].

[20] C. Lunardini and A. Y. Smirnov, JCAP **0306**, 009 (2003) [arXiv:hep-ph/0302033].

[21] K. Hirata *et al.* [KAMIOKANDE-II Collaboration], Phys. Rev. Lett. **58** (1987) 1490.

[22] R. M. Bionta *et al.*, Phys. Rev. Lett. **58** (1987) 1494.

[23] M. K. Sharp, J. F. Beacom and J. A. Formaggio, Phys. Rev. D **66** (2002) 013012 [arXiv:hep-ph/0205035].

[24] S. Choubey, D. Majumdar and K. Kar, J. Phys. G **25** (1999) 1001 [arXiv:hep-ph/9809424]; G. Dutta, D. Indumathi, M. V. Murthy and G. Rajasekaran, Phys. Rev. D **61** (2000) 013009; Phys. Rev. D **64** (2001) 073011 [arXiv:hep-ph/0101093]; I. Gil-Botella and A. Rubbia, JCAP **0310**, 009 (2003) [arXiv:hep-ph/0307244].

[25] C. Lunardini and A. Y. Smirnov, Nucl. Phys. B **616**, 307 (2001) [arXiv:hep-ph/0106149].

[26] K. Takahashi and K. Sato, Phys. Rev. D **66**, 033006 (2002) [arXiv:hep-ph/0110105].

[27] A. S. Dighe, M. T. Keil and G. G. Raffelt, JCAP **0306**, 006 (2003) [arXiv:hep-ph/0304150].

[28] A. S. Dighe, M. Kachelriess, G. G. Raffelt and R. Tomas, arXiv:hep-ph/0311172.

[29] H. Minakata, H. Nunokawa, R. Tomas and J. W. F. Valle, Phys. Lett. B **542**, 239 (2002) [arXiv:hep-ph/0112160].

[30] V. Barger, D. Marfatia and B. P. Wood, Phys. Lett. B **547**, 37 (2002) [arXiv:hep-ph/0112125].

[31] Proposal for US participation in KamLAND, March 1999.

[32] L. Cadonati, F. P. Calaprice and M. C. Chen, Astropart. Phys. **16**, 361 (2002) [arXiv:hep-ph/0012082].

[33] J. F. Beacom, W. M. Farr and P. Vogel, Phys. Rev. D **66**, 033001 (2002) [arXiv:hep-ph/0205220].

[34] S. L. Shapiro and S. A. Teukolsky, Black Holes, White Dwarfs, and Neutron Stars (Wiley, New York, 1983).

[35] K. Langanke, P. Vogel and E. Kolbe, Phys. Rev. Lett. **76**, 2629 (1996) [arXiv:nucl-th/9511032].

[36] T. Totani, K. Sato, H. E. Dalhed and J. R. Wilson, Astrophys. J. **496**, 216 (1998) [arXiv:astro-ph/9710203].

[37] M. T. Keil, G. G. Raffelt and H. T. Janka, Astrophys. J. **590** (2003) 971 [arXiv:astro-ph/0208035].

[38] G. G. Raffelt, M. T. Keil, R. Buras, H. T. Janka and M. Rampp, arXiv:astro-ph/0303226.

[39] H. T. Janka, Astron. Astrophys. **224**, 49 (1989); P.M. Giovanoni, P.C. Ellison and S.W. Bruenn, Astrophys. J. **342**, 416 (1989).

[40] D. Notzold, Phys. Lett. B193(1987) 127.

[41] T. K. Kuo and J. Pantaleone, Phys. Rev. D37(1988) 298.

[42] G. E. Brown, H. A. Bethe and G. Baym, nucl. Phys. A 375 (1982) 481.

[43] C. Athanassopoulos *et al.*, (The LSND Collaboration) Phys. Rev. Lett. **77**, 3082 (1996); C. Athanassopoulos *et al.*, (The LSND Collaboration) Phys. Rev. Lett. **81**, 1774 (1998).

[44] G. Dutta, D. Indumathi, M. V. Murthy and G. Rajasekaran, Phys. Rev. D **62** (2000) 093014 [arXiv:hep-ph/0006171].

[45] B. Pontecorvo, Zh. Eksp. Teor. Fiz. **33** (1957) 549, and **34** (1958) 247; Z. Maki, M. Nakagawa and S. Sakata, Prog. Theor. Phys. 28 (1962) 870.

[46] T. K. Kuo and J. Pantaleone, Rev. Mod. Phys. **61**, 937 (1989); T. K. Kuo and J. Pantaleone, Phys. Rev. D **37**, 298 (1988).

[47] S. T. Petcov, Phys. Lett. B **200**, 373 (1988).

[48] G. L. Fogli, E. Lisi, D. Montanino and A. Palazzo, Phys. Rev. D **65**, 073008 (2002) [Erratum-ibid. D **66**, 039901 (2002)] [arXiv:hep-ph/0111199].

[49] S. Choubey and K. Kar, arXiv:hep-ph/0212326.

[50] S. Choubey, S. Goswami, K. Kar, H. M. Antia and S. M. Chitre, Phys. Rev. D **64**, 113001 (2001) [arXiv:hep-ph/0106168].

[51] S. T. Petcov, Phys. Lett. B **434**, 321 (1998) [arXiv:hep-ph/9805262].

[52] P. Vogel and J. F. Beacom, Phys. Rev. D **60**, 053003 (1999) [arXiv:hep-ph/9903554].

[53] J. Engel, E. Kolbe, K. Langanke and P. Vogel, Phys. Rev. C **54**, 2740 (1996) [arXiv:nucl-th/9606031]; E. Kolbe, F. K. Thielemann, K. Langanke and P. Vogel, Phys. Rev. C **52**, 3437 (1995); E. Kolbe, K. Langanke and S. Krewald, Phys. Rev. C **49**, 1122 (1994).

[54] F.v. Feilitzsch, L. Oberauer and W. Potzel, private communication; L. Oberauer, talk at TAUP 2003, September 5–9, 2003, Seattle, Washington, *http://mocha.phys.washington.edu/taup2003/*; L. Oberauer, talk at International Workshop on: "Neutrino Oscillations in Venice", December 3–5, 2003, Venice, *http://axpd24.pd.infn.it/NO-VE/NO-VE.html*